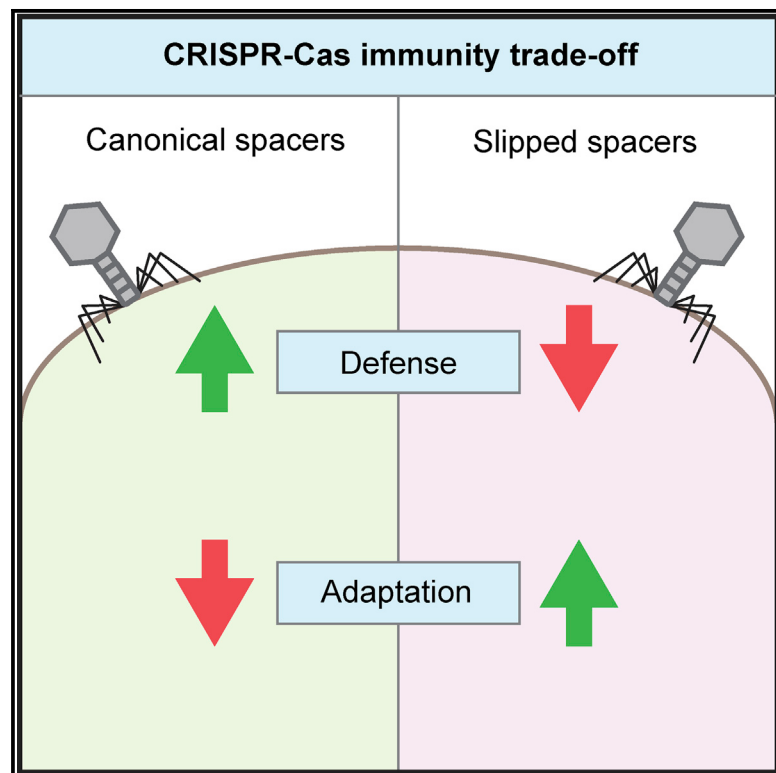


Cell Host & Microbe

Imprecise Spacer Acquisition Generates CRISPR-Cas Immune Diversity through Primed Adaptation

Graphical Abstract



Authors

Simon A. Jackson, Nils Birkholz,
Lucía M. Malone, Peter C. Fineran

Correspondence

simon.jackson@otago.ac.nz (S.A.J.),
peter.fineran@otago.ac.nz (P.C.F.)

In Brief

CRISPR-Cas prokaryotic immune systems acquire genetic memories, termed spacers, to facilitate defense against phages and mobile genetic elements. Jackson et al. (2018) discover that imprecisely acquired (slipped) spacers are less effective for defense but enhance the acquisition of new spacers, which pre-emptively increases immune diversity before phage escape mutants arise.

Highlights

- Imprecisely acquired (slipped) spacers are impaired for CRISPR-Cas immunity
- -1 and $+1$ slipped spacers stimulate primed CRISPR adaptation
- Slipped spacers enhance priming before phage escape mutations arise
- Slipping enhances CRISPR-Cas resilience to phage mutation by increasing immune diversity



Imprecise Spacer Acquisition Generates CRISPR-Cas Immune Diversity through Primed Adaptation

Simon A. Jackson,^{1,*} Nils Birkholz,¹ Lucía M. Malone,¹ and Peter C. Fineran^{1,2,*}

¹Department of Microbiology and Immunology, University of Otago, Dunedin 9054, New Zealand

²Lead Contact

*Correspondence: simon.jackson@otago.ac.nz (S.A.J.), peter.fineran@otago.ac.nz (P.C.F.)

<https://doi.org/10.1016/j.chom.2018.12.014>

SUMMARY

Many prokaryotes possess CRISPR-Cas adaptive immune systems to defend against viruses and invading mobile genetic elements. CRISPR-Cas immunity relies on genetic memories, termed spacers, for sequence-specific recognition of infections. The diversity of spacers within host populations is important for immune resilience, but we have limited understanding of how CRISPR diversity is generated. Type I CRISPR-Cas systems use existing spacers to enhance the acquisition of new spacers through primed CRISPR adaptation (priming). Here, we present a pathway to priming that is stimulated by imprecisely acquired (slipped) spacers. Slipped spacers are less effective for immunity but increase priming compared with canonical spacers. The benefits of slipping depend on the relative rates of phage mutation and adaptation during defense. We propose that slipped spacers provide a route to increase population-level spacer diversity that pre-empts phage escape mutant proliferation and that the trade-off between adaptation and immunity is important in diverse CRISPR-Cas systems.

INTRODUCTION

Many bacteria and archaea possess CRISPR-Cas adaptive immune systems, which provide sequence-specific defenses against bacteriophage infections and invading mobile genetic elements (MGEs) (Barrangou et al., 2007; Marraffini and Sontheimer, 2008). There are many diverse CRISPR-Cas systems, which are classified into six main types and multiple subtypes (Makarova et al., 2015; Shmakov et al., 2015; Koonin et al., 2017). CRISPR-Cas defense uses genetic “memories” of prior infections, in the form of spacers stored within CRISPR arrays, to recognize foreign nucleic acids and elicit an immune response termed interference (Barrangou et al., 2007; Brouns et al., 2008). Since spacer sequences determine CRISPR-Cas target specificity, immunity can be updated by the acquisition of new spacers via a process termed CRISPR adaptation (Barrangou

et al., 2007; Horvath et al., 2008; Amitai and Sorek, 2016; Sternberg et al., 2016; Jackson et al., 2017).

Phage and MGE variants with genetic mutations can escape CRISPR-Cas interference facilitated by existing spacers (Deveau et al., 2008; Semenova et al., 2011). In response, hosts constantly update their spacer repertoires (Andersson and Banfield, 2008). Diversity in CRISPR loci, with regard to the number of spacers as well as their sequence, is important for assuring effective immunity in both individual hosts and populations (Barrangou et al., 2007; Deveau et al., 2008; Held et al., 2010; Childs et al., 2014; van Houte et al., 2016). More spacers in an individual that target an invader decrease the probability of escape mutant proliferation because all spacers must be evaded (Levin et al., 2013). At a population level, invaders that escape spacers within one host will be unable to replicate on neighboring strains that possess different spacers (van Houte et al., 2016; Chabas et al., 2018). Despite the importance of CRISPR diversity, our current understanding of the mechanisms underlying its generation is limited.

Type I systems are the most widespread CRISPR-Cas systems and consist of seven subtypes (Makarova et al., 2015). Multiple type I systems have been shown to increase their spacer diversity by primed CRISPR adaptation (priming), which reinforces immunity during infections (Swarts et al., 2012; Semenova et al., 2016; Staals et al., 2016) and in response to escape mutants (Datsenko et al., 2012; Swarts et al., 2012). Priming occurs even if the invader is heavily mutated or divergent (Fineran et al., 2014). Spacers in type I systems are typically acquired from foreign DNA next to conserved sequences, termed protospacer-adjacent motifs (PAMs), which are required to distinguish invaders from the host CRISPR loci (Mojica et al., 2009; Leenay et al., 2016). In our previous study of priming by the type I-F system in *Pectobacterium atrosepticum*, we found that approximately 1 in 15 new spacers are not selected from adjacent to canonical (GG) PAMs (Figure 1) (Richter et al., 2014; Staals et al., 2016). Instead, the majority of these non-canonical spacers are acquired from one nucleotide upstream or downstream of the correct PAM position. This imprecision in PAM selection is termed “slipping” and has also been noted in type I-B, I-C, and I-E CRISPR-Cas systems (Swarts et al., 2012; Savitskaya et al., 2013; Shmakov et al., 2014; Li et al., 2017; Rao et al., 2017). Despite evidence for the widespread conservation of slipping during spacer acquisition, it is not known whether slipped spacers have any role in CRISPR-Cas immunity.



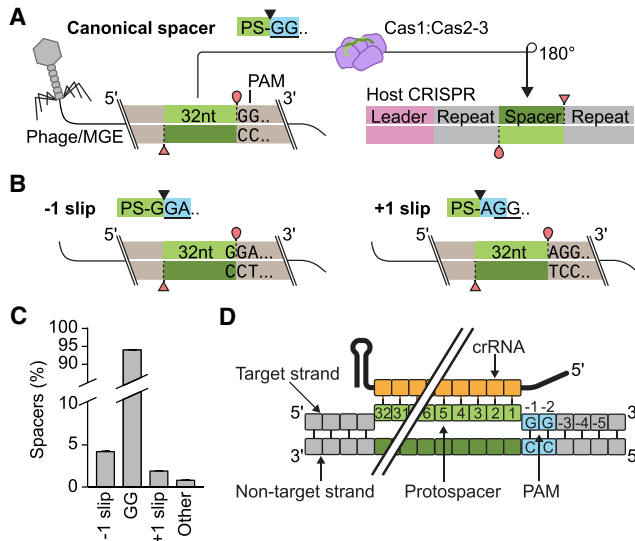


Figure 1. Schematic and Nomenclature of Slipping in Type I-F CRISPR-Cas Systems

(A) In type I-F CRISPR-Cas systems, canonical spacers are obtained from protospacers (PS) immediately adjacent to di-nucleotide (GG) PAMs. The Cas1:Cas2-3 complex (the Cas2-3 fusion protein is unique to type I-F systems) catalyses integration of pre-spacer substrates into host CRISPR arrays (Fagerlund et al., 2017).

(B) Imprecision during spacer acquisition (slipping) resulting in GN or NG PAMs.

(C) The frequency of slipping in the *P. atrosepticum* type I-F system. Data are the mean \pm SEM ($n = 6$) from Staal et al. (2016).

(D) Schematic of target recognition in the type I-F system, detailing the numbering convention for protospacer and PAM positions. The protospacer, which is complementary to the spacer, is denoted on the target strand (Westra et al., 2012). For compactness, the diagram has been truncated by removal of positions 7–30.

Here, we show that slipped spacers in type I-F and I-E CRISPR-Cas systems are impaired for interference but strongly stimulate primed CRISPR adaptation. Importantly, we demonstrate that they promote enhanced priming compared with priming facilitated by canonical spacers during interference. As such, priming by slipped spacers provides a mechanism to increase the rate of CRISPR diversification that pre-empts phage escape, thereby aiding the establishment of population-level immune resilience. By modeling the impact of the trade-off between efficient immunity and CRISPR adaptation, we determine that slipping represents a bet-hedging strategy that may be broadly applicable across CRISPR-Cas systems.

RESULTS

-1 Slipped Spacers Stimulate Primed CRISPR Adaptation

To study the function of slipped spacers, we used the native type I-F host *P. atrosepticum*. -1 slips result in the incorporation of part of the PAM in the spacer itself, i.e., a C at the 5' end of the integrated spacer (Figure 1B). Since spacer efficiency can depend on their sequence (Xue et al., 2015), we selected three endogenous spacers from the CRISPR1 array (spacers 4, 9, and 19) that begin with C and might have been derived

during -1 slips. We constructed mobilizable plasmids with protospacers matching these spacers, then tested their ability to provoke interference in conjugation assays in *P. atrosepticum*. Positive control plasmids that possessed protospacers engineered to represent non-slipped spacer targets (GG PAMs) elicited strong interference, observed as a reduction in the transconjugant frequency, compared with an untargeted control lacking any protospacer (no PS) (Figure 2A). By contrast, we observed only minor interference for some of the plasmids containing protospacer targets of -1 slipped spacers in the wild-type (WT) recipient; however, this was not observed in a mutant recipient that cannot prime (Cas1^{D269A}) (Figures 2A and S1). These data suggest that the apparent interference by -1 slips in the WT strain resulted from priming during the conjugation assay, followed by plasmid interference using the new spacers. To further investigate priming by -1 slipped spacers, we tracked plasmid loss in *P. atrosepticum* populations using flow cytometry. Cells that become cured of the plasmids typically do so after the primed acquisition of additional plasmid-targeting spacers (Swarts et al., 2012; Richter et al., 2014). Most -1 slip plasmids were rapidly cleared, whereas the plasmid lacking a protospacer was stable (Figure 2B). Moreover, robust CRISPR adaptation was observed in the -1 slip samples (Figures 2C and 2D). To investigate whether the effects of -1 slipped spacers stemmed from their "effective" GN mutant PAMs (Figure S2A), we also tested spacer 1 (which does not begin with C) as a representative of target escapes compared with -1 slips (Figure S2B). These data were similar to the outcomes observed for -1 slipped spacers (Figure 2A), suggesting that -1 slipped spacers function analogous to PAM mutants. Overall, these findings demonstrate that -1 slipped type I-F spacers do not facilitate direct interference but strongly stimulate primed CRISPR adaptation.

+1 Slipped Spacers Stimulate Primed CRISPR Adaptation

To study the function of +1 slipped spacers, where an additional nucleotide occurs between the protospacer and the GG (Figure 1B), we used a protospacer matching spacer 1 (PS1) with either an A, C, or T inserted between the protospacer and GG PAM (Figure 2E). As a comparison, we also tested NG PAM mutations with the [-1] position changed to A, C, or T. In contrast to the strong interference of the canonical target plasmid (PS1 with a GG PAM), none of the +1 slip or PAM mutant plasmids was subject to direct interference. The apparent low level of interference with the +1 slip CGG PAM was due to priming because it was Cas1-dependent. In the priming assay, +1 slipped plasmids were rapidly cleared from the host, concomitant with CRISPR expansion (Figures 2F and 2G). The +1 slipped plasmids were cleared more rapidly than the corresponding [-1] position PAM "escape" mutants (e.g., TGG or CGG compared with TG or CG PAMs). Our findings demonstrate that these +1 slipped spacers are not functional for CRISPR-Cas interference but typically stimulate strong primed CRISPR adaptation.

Establishment of CRISPR Diversity by Slipped Spacers

We theorized that priming stimulated by slipped spacers might enhance the generation of immune diversity during subsequent

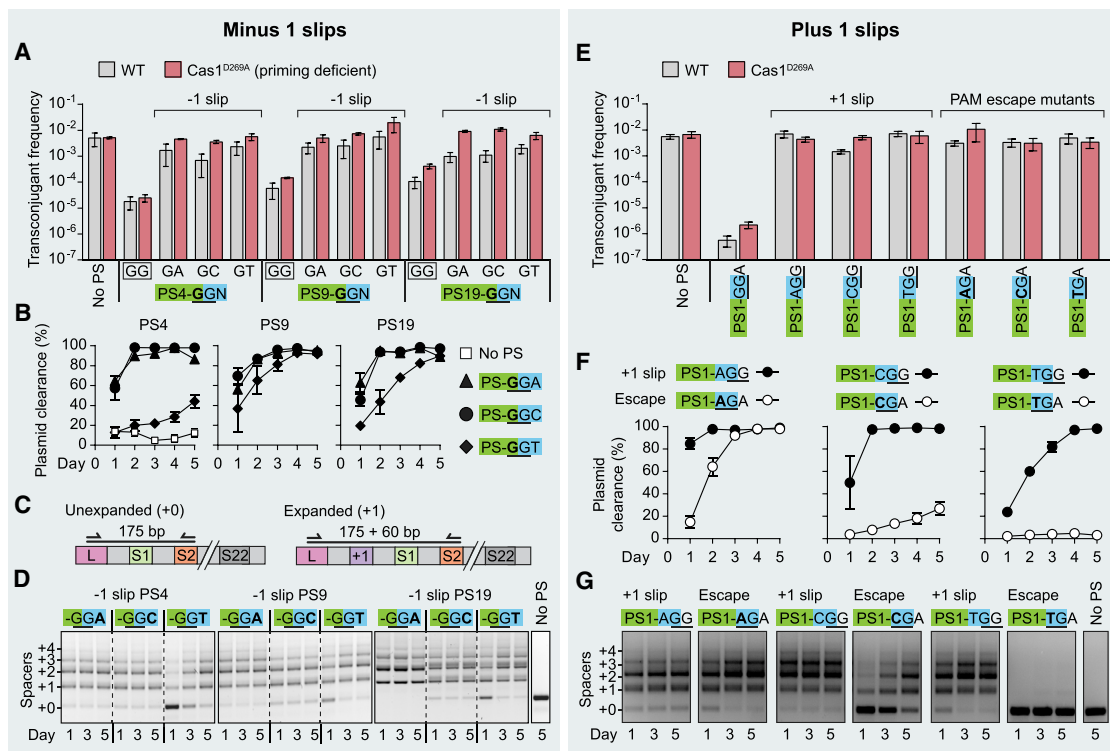


Figure 2. Slipped Spacers Stimulate Primed CRISPR Adaptation

(A) Plasmid interference of wild-type (WT) and Cas1^{D269A} *P. atrosepticum* recipients infected with either an untargeted (no PS) control plasmid, canonical target (GG PAM) plasmids or plasmids with targets matching –1 slipped spacers. In the x-axis schematics, the canonical PAM (GG) is underlined, and the protospacer-proximal dinucleotide, position [–1, –2], is colored blue.

(B) Clearance of plasmids from transconjugants infected in (A), determined by flow cytometry detecting a plasmid-borne fluorescent reporter. Plasmids with canonical PAMs (GG) could not be measured because they provoked direct interference, which results in genetically unstable transconjugants.

(C) Schematic of the CRISPR expansion PCR, where the leader-proximal end (L) of the host CRISPR is amplified.

(D) Samples taken from (B) at the times indicated were examined for primed CRISPR adaptation by PCR. The y-axis indicates the number of new spacers acquired.

(E) Plasmid interference with a canonical target (GG PAM) plasmid, +1 slipped plasmids or single nucleotide PAM mutants.

(F) Plasmid clearance from WT transconjugants infected with plasmids in (E) was determined by flow cytometry detecting a plasmid-borne fluorescent reporter. The canonical (GG PAM) plasmid was not tested because it was subject to strong interference, making transconjugants genetically unstable.

(G) Samples taken from (F) at the indicated times and examined by PCR for spacer acquisition. Data shown in (A), (B), (E), and (F) are the mean ± SEM ($n \geq 3$).

infections, perhaps to a greater extent than by the positive feedback loop due to primed CRISPR adaptation from canonical spacers (Swarts et al., 2012; Semenova et al., 2016; Staals et al., 2016). To examine this idea, we developed an assay termed “pestering” that mimics recurrent encounters with foreign genetic material. In this assay, cell populations are subjected to invasion by mobile plasmids through iterative conjugation (Figure 3A). The pestering plasmids either lacked a protospacer (no PS) or contained PS1 or PS9 and PAMs representing targets of canonical or slipped spacers. As expected, CRISPR adaptation was not observed in the populations pestered with the no protospacer control, but priming did occur from the canonical (GG PAM) plasmids and for all slipped samples (Figure 3B). To quantify CRISPR adaptation, we developed a deep sequencing approach that allows normalization between samples on a per cell basis and accounts for amplicon size biases (Figure S3A). Pestering with the non-slipped (GG PAM) plasmids stimulated CRISPR adaptation in ~23% of the population. By screening for the plasmid in the no protospacer control

populations, we determined that >30% of *P. atrosepticum* cells were infected during the assay. Due to non-CRISPR factors, such as innate defenses, this is likely to represent the minimum proportion of cells that encountered the plasmid (Figure S3B). Therefore, ~70% of cells inferred to be infected with the canonical spacer targets underwent priming, with most arrays expanding by only one spacer (Figure 3C). The proportion of expanded CRISPR loci in the slipped populations was generally greater than in the non-slipped samples. Importantly, slipping substantially increased the number of new spacers acquired in each expanded CRISPR array. This increase was reflected in both the number and combination of unique spacers in the populations (Figures 3D, 3E, S3C, and S3D). As such, the diversity of spacers and CRISPR loci in the slipped samples was higher than in the non-slipped samples (Figures S3E and S3F).

Next, we mapped the new spacers to the corresponding protospacer locations on the plasmids from which the spacers were acquired (Figure 3F). Interestingly, this mapping revealed that, compared with canonical spacers, slipped spacers stimulated

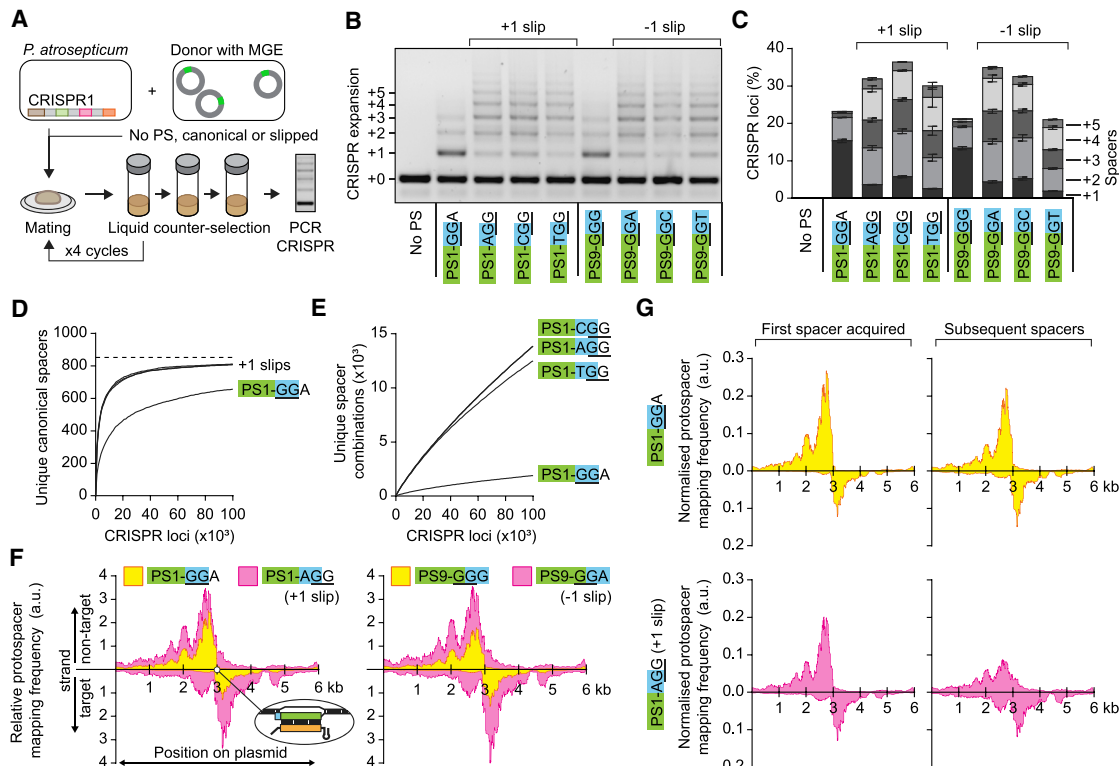


Figure 3. Establishment of CRISPR Diversity by Slipped Spacers

- (A) Schematic of the recurrent infection “pestering” assay.
 - (B) CRISPR expansion in pestered cell populations, determined by PCR.
 - (C) The proportion of cells that underwent CRISPR adaptation, determined by quantitative deep sequencing of expanded arrays.
 - (D) Spacer richness (unique canonical spacers) in the pestered populations. The dashed line represents the maximum potential of unique canonical spacers, based on the plasmid sequence.
 - (E) Unique spacer combinations, irrespective of their order within arrays. Equivalent data for PS9 are supplied in Figures S3C–S3F.
 - (F) Mapping of protospacers corresponding to new spacers acquired from the plasmids. The target protospacer is positioned at the center of the plasmid (3 kb) (left-hand inset). Data were smoothed by rolling-sum windows of 250 bp, resulting in an arbitrary density scale (a.u.). Protospacers mapped to the non-target and target strand are plotted above and below the x axes, respectively.
 - (G) Protospacer maps, as in (F), but normalized to the total number of protospacers in each sample and separated into the first and subsequent new spacers. Similar trends in (F) and (G) were observed for all samples (Figures S3G and S3H).
- Data shown in (C) are the mean \pm SEM ($n = 3$), and data in (D), (E), (F), and (G) are the mean ($n = 3$).

CRISPR adaptation from more widespread plasmid locations, with broader and more even strand distributions. This broader distribution was not due to the first acquired spacers for slipped versus non-slipped samples, which displayed similar mapping distributions (Figure 3G). Instead, differences in the total distributions arise from spacers acquired after the first new spacer (Figure 3G). These results indicate that there is no apparent distinction between the mechanism that leads to the primed acquisition of the first new spacers for canonical targets versus targets of slipped spacers. Instead, secondary priming events subsequent to the first spacer acquisition, presumably driven by the new canonical spacers, contribute to increases in both the diversity and number of spacers acquired as a result of slipping-stimulated primed CRISPR adaptation. These data are in agreement with our previous mechanistic analyses of type I-F priming (Staals et al., 2016). The net result is that, compared with canonical spacers, slipped spacers lead to more rapid establishment of CRISPR diversity in cell populations that are subject to recurring infections.

Slipping Establishes CRISPR Diversity in Type I-E Systems

To explore whether slipped spacers also generate CRISPR diversity by priming in other type I CRISPR-Cas systems and in different bacteria, we examined the type I-E system in *Serratia* sp. ATCC 39006. This bacterium possesses three CRISPR-Cas systems (types I-E, I-F, and III-A) (Fineran et al., 2013; Patterson et al., 2016). The most common slipping events observed in type I-E systems are +1 slips (Figures 4A and 4B) (Savitskaya et al., 2013; Shmakov et al., 2014). To examine if +1 slips elicit interference, we tested plasmid conjugation with protospacers (PS1 and PS2) matching either spacer 1 or spacer 2 in the *Serratia* type I-E CRISPR1 array. As expected, a plasmid lacking any protospacer (no PS) infected a high proportion of the recipient population, whereas protospacer-containing controls with canonical (CTT) PAMs were subject to robust interference (Figure 4C). The +1 slip plasmids with ACTT and GCTT PAMs were not subject to interference, whereas CCTT and TCTT were targeted to differing extents in a spacer-dependent manner.

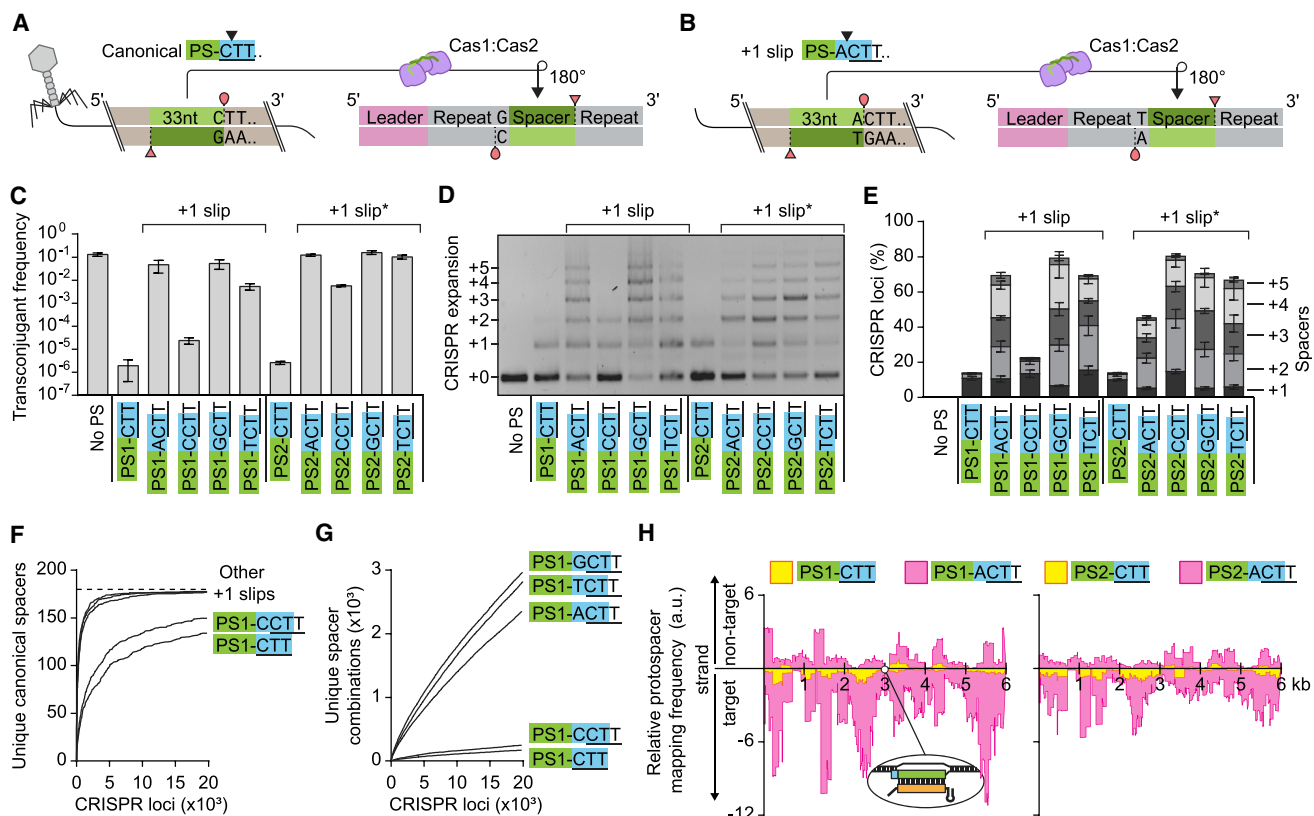


Figure 4. Slipping Establishes CRISPR Diversity in Type I-E Systems

- (A) Schematic of canonical type I-E spacer acquisition. The last nucleotide of each repeat is derived from the cytosine of the canonical CTT PAM.
 - (B) Schematic of +1 slip events in type I-E systems, which result in the incorporation of the base preceding the CTT PAM (Swarts et al., 2012; Savitskaya et al., 2013).
 - (C) Plasmid interference data. *In *Serratia* the second type I-E CRISPR1 repeat ends with T (ordinarily G), which is consistent with a +1 slipped spacer (corresponding with PS2).
 - (D) Expansion of the type I-E CRISPR in populations pestered by recurrent plasmid infections.
 - (E) CRISPR expansion in the pestering assay, determined by quantitative deep sequencing.
 - (F) Spacer richness (unique canonical spacers) for pestered cell populations. The dashed line represents the maximum potential of unique canonical spacers.
 - (G) Unique spacer combinations, irrespective of their order within arrays. Equivalent data for PS2 are in Figure S4B–S4E.
 - (H) Maps of protospacers corresponding to new spacers acquired from the plasmids. The target protospacer is positioned at the center of the plasmid (3 kb) (left-hand inset). Data were smoothed by rolling-sum windows of 250 bp, resulting in an arbitrary density scale. Additional data are in Figure S4F.
- Data shown in (C) and (E) are the mean \pm SEM ($n \geq 3$), and data in (F), (G), and (H) are the mean ($n = 3$).

Therefore, +1 slips in a type I-E system either impair or alleviate interference.

To examine whether slipping in the type I-E system stimulated priming, we applied the pestering assay to *Serratia*. CRISPR adaptation was observed for all populations pestered with protospacer-containing plasmids (Figure 4D). Strikingly, canonical targets resulted mostly in the acquisition of only one new spacer, whereas +1 slips typically resulted in the acquisition of several new spacers. In *Serratia*, the plasmid infection rate, determined using the untargeted plasmid, was >50% (Figure S4A). Quantitative deep-sequencing of the expanded CRISPRs revealed that substantially more cells in the slipped populations underwent CRISPR adaptation compared with the canonical populations (Figure 4E). Moreover, the proportion of expanded arrays containing two or more new spacers was greatly increased by slipping-stimulated CRISPR adaptation. There were also more unique plasmid-targeting spacers in the slipped populations

(Figure 4F) and a greater richness in CRISPR loci (Figure 4G). Moreover, the diversity of both spacers and CRISPR loci was enhanced in the slipped samples (Figures S4D and S4E). The new spacers in the slipped samples originated from a broader distribution of locations on the plasmids than that observed with canonical targets (Figures 4H and S4F). Overall, these data for the *Serratia* type I-E system agree with our findings in the *P. atrosepticum* type I-F system, demonstrating that the enhancement of CRISPR diversity promoted by priming from slipped spacers is likely to be a widespread mechanism in type I CRISPR-Cas systems and in different bacteria.

Slipped Spacers Increase CRISPR Diversity during Phage Infection

An important question is whether slipping-stimulated primed CRISPR adaptation also occurs during phage infection. To address this question, we used a *Serratia* phage, JS26, to

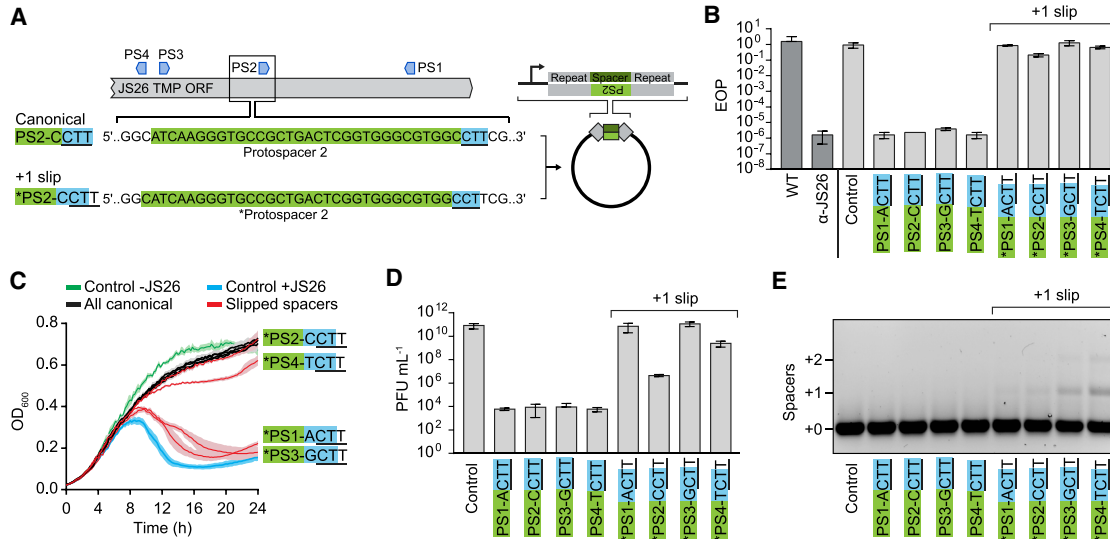


Figure 5. Slipped Spacers Increase CRISPR Diversity during Phage Infection

(A) Schematic of the plasmid-borne mini-CRISPR loci harboring canonical or slipped spacers for the *Serratia* type I-E system. The spacers target JS26 within the tape measure protein (TMP) coding region.

(B) Phage defense provided by canonical and slipped spacers, measured as the EOP relative to the negative control spacer that does not target JS26. WT *Serratia* and a bacteriophage-insensitive mutant that possesses a canonical spacer in the native CRISPR loci (α -JS26) are shown for comparison to the plasmid-borne mini-CRISPR strains.

(C) Time courses of growth in populations infected with JS26; MOI = 0.01. The shaded area bounding each line shows the SEM.

(D) Phage titers in infected populations (C) at the 24 h endpoint.

(E) CRISPR adaptation in infected populations (C) at the 24 h endpoint.

Data for type I-F spacers are included in Figure S5. Data shown are the mean \pm SEM ($n \geq 3$).

directly compare canonical and slipped spacers expressed from plasmid-borne mini-CRISPR loci (Figure 5A). In efficiency of plaquing (EOP) assays, canonical spacers provided robust defense against JS26, compared with a control spacer that does not target JS26, whereas slipped spacers failed to provide effective immunity (Figure 5B). In liquid cultures, canonical type I-E spacers provided population-level protection compared with the negative control spacer populations (Figure 5C). All slipped spacers provided some protection compared with the non-specific control, ranging from nearly complete to minor (Figure 5C). For all samples with canonical spacers, phage titers were relatively low at the 24 h end point, whereas in the slipped and negative control populations the titers were higher (Figure 5D). For some slipped spacers, phage proliferation was reduced compared with the negative control lacking immunity against JS26 (Figure 5D). Importantly, slipped populations acquired more spacers in response to JS26 infection when compared with undetectable spacer acquisition in populations containing the non-specific or canonical spacers (Figure 5E). There was no clear linear relationship between impaired defense and CRISPR adaptation stimulated by slipped spacers (Figure 5C), suggesting that the balance between defense and CRISPR adaptation may be spacer-specific during phage infections. The *Serratia* type I-F system displayed similar but subtler trends (Figure S5). Overall, these data support a model for the slipping-induced establishment of CRISPR diversity in response to both plasmid and phage infections.

Slipping Extends Immune Resilience to Rapidly Mutating Phages by Increasing CRISPR Diversity

Our phage and plasmid infection data highlight both the potential costs (reduced initial interference) and fitness benefits (subsequent increased CRISPR diversity and immunity) associated with slipped spacers. To further examine these trade-offs, we developed an agent-based model to probe the population-level impact of slipping. The objective of this approach was to overcome experimental limitations of our host-phage system, including non-CRISPR immunity (e.g., receptor mutants), thus allowing us to probe when and how slipped spacers might impact CRISPR-phage coevolution. In addition, the model allowed us to directly compare the presence and absence of slipping, which is not feasible with an experimental system. The model consists of a spatially structured bacterial community that is infected with phages (Figure 6A), where hosts possess CRISPR-Cas systems and phages randomly acquire mutations that facilitate escape from immunity. During infections, new spacers (either canonical or slipped) can be acquired by priming facilitated by existing canonical or slipped spacers. Based on the findings of a previous experimental study of CRISPR diversity and phage extinction in a relatively simple system (van Houte et al., 2016), we monitored spacer richness in the community and allowed the system to progress until either phages or hosts were driven to extinction (Figure 6B). To determine the population-level impacts of priming from slipped spacers compared with canonical spacers, we ran simulations with slipping at either 0 or 5% of new spacers. We modeled the general behavior of

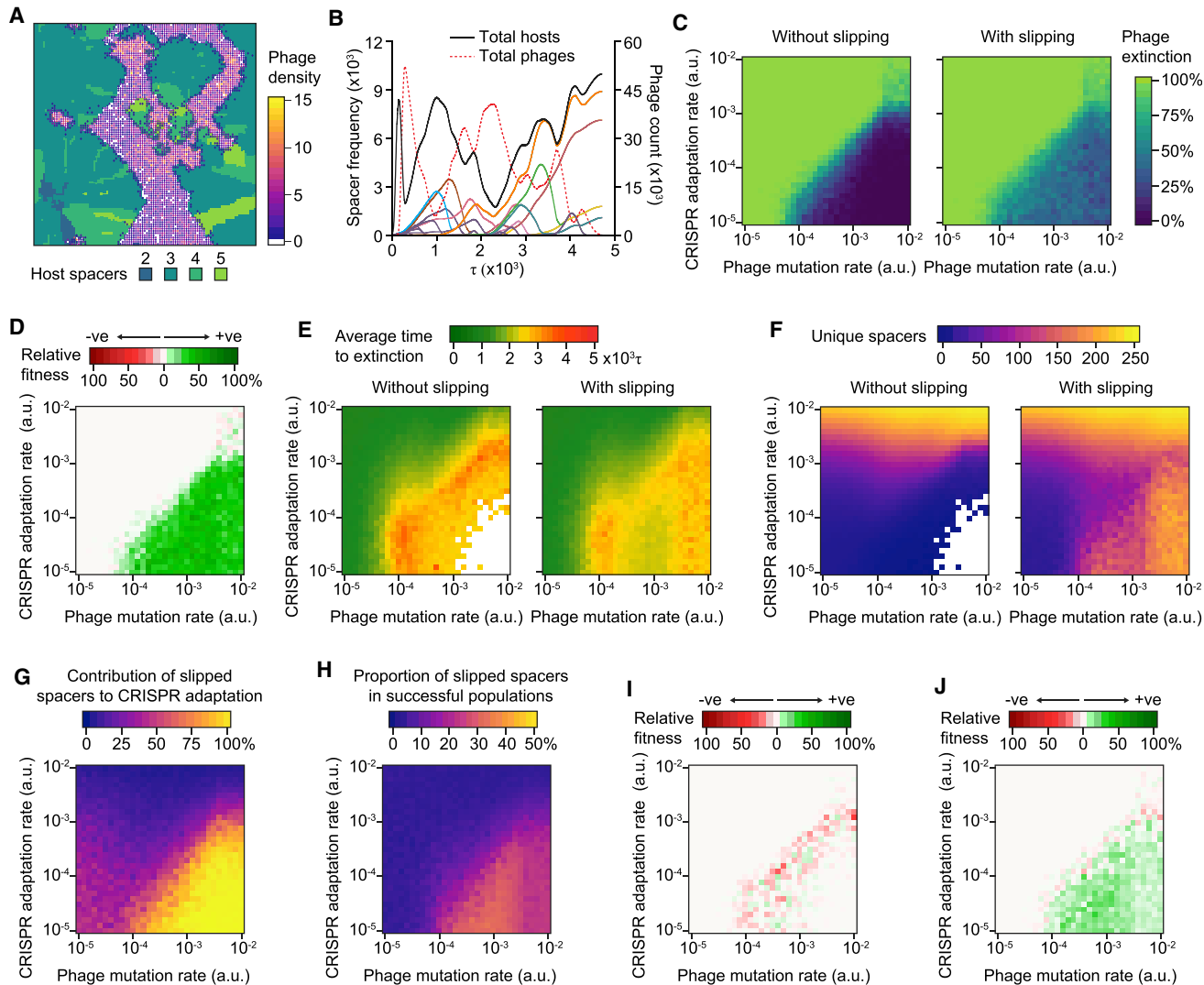


Figure 6. Slipping Extends Immune Resilience to Rapidly Mutating Phages by Increasing Spacer Diversity

- (A) A representative example of the host-phage population structure at $\tau = 1,000$. Hosts are colored according to the number of spacers in their CRISPR loci.
- (B) A representative plot of the population dynamics throughout a simulation. The total host and phage populations are shown by black and dashed red lines, respectively. The colored lines represent the frequency of different spacers within the host population.
- (C) The proportion of trials where phages were driven to extinction as a function of the phage mutation and host CRISPR adaptation rates with the slipping frequency set at 0 or 5% of acquired spacers. For each combination of parameters $n = 100$ simulations.
- (D) The relative fitness for slipping versus non-slipping outcomes, represented as the difference in phage extinction proportions observed in (C).
- (E) The mean simulation times (τ) until phage extinction for the data in (C). These data exclude cases where hosts were driven to extinction.
- (F) The average spacer richness (number of unique spacers in the population) at the point of phage extinction for the data in (C). To prevent artificial inflation in the slipping samples, only canonical spacers are counted.
- (G) The proportion of spacers in successful host populations that were acquired via priming stimulated by slipped spacers.
- (H) The frequency of slipped spacers observed in populations upon phage extinction.
- (I) The relative fitness between slipping and non-slipping models when slipped spacers were set as non-functional.
- (J) The relative fitness between slipping and non-slipping models when the probability of priming with slipped spacers was 1%. To reduce computational time, the data presented in (I) and (J) were obtained using a reduced grid size (75 × 75). We also examined the robustness of our findings by testing additional model parameters, with similar results (Figure S6).

defense facilitated by slipped compared with canonical spacers on our experimental data, i.e., slipped spacers were impaired for interference but stimulated stronger priming than canonical spacers (Table S1). Initially, we set slipped spacers to provide a 10% chance of priming and survival and a 90% chance that infections would lead to lysis and phage release. Because we were

unable to derive these values from experimental data, we also confirmed the modeling results were consistent over a wide range of values (Figures S6A–S6C and described below). Since any benefits of priming by slipped spacers also depend on the efficiency of CRISPR adaptation with canonical spacers, we ran simulations with varying probabilities of priming by canonical

spacers compared with varying probabilities that phage escape mutations arise. A detailed description of the model is provided in the [STAR Methods](#).

In the absence of slipping, we observed two main outcomes that were dominated by either phage or host extinction. These outcomes depended on the relative rates of phage mutation and the chance of CRISPR adaptation during interference with canonical spacers ([Figure 6C](#)). These results are consistent with previous simulations of CRISPR immunity showing that increased viral mutation rates decrease the efficacy of CRISPR immunity ([Weinberger et al., 2012](#)). For example, when CRISPR adaptation was high, relative to the phage mutation rate, phages were typically driven to extinction and vice versa. In the presence of slipping for 5% of spacers, the conditions that were previously dominated by phages (i.e., high phage mutation and low priming during interference) displayed increased success of bacterial populations ([Figures 6C and 6D](#)). This suggests that slipping is advantageous when the rate of primed CRISPR adaptation by canonical spacers is insufficient to keep pace with phage escape. Slipping also accelerated the rate of phage extinction, most notably when competition between hosts and phages was greatest ([Figure 6E](#)). In agreement with our plasmid and phage experiments, the spacer diversity that drove phages to extinction was increased by slipped spacers ([Figure 6F](#)), and this diversity was the direct result of priming by slipped spacers in members of these populations ([Figure 6G](#)). In addition, we observed positive selection for slipped spacers under conditions when slipping provided the strongest positive impact on population fitness ([Figure 6H](#)). To reveal conditions where slipped spacers might have a negative influence on population fitness, we also ran the model with slipped spacers set as non-functional, i.e., not providing immunity or stimulating priming ([Figure 6I](#)). In general, negative impacts were most apparent in populations with high competition between hosts and phages. By varying the probability of CRISPR adaptation by slipped spacers, we observed that the population-level benefits of slipping were maintained at low priming and survival rates (e.g., 1%) ([Figures 6J and S6C](#)) and also when priming by slipped spacers only resulted in one new spacer being acquired ([Figure S6D](#)).

Overall, our agent-based modeling shows that the diversity-generating effect of slipped spacers has the highest impact when the rate of phage mutation exceeds the rate of primed CRISPR adaptation during interference with canonical spacers. This highlights the critical trade-off between spacers that provide efficient defense and the ability to undergo CRISPR adaptation. In agreement, our experimental data showed that spacers that are very efficient for immunity reduce primed CRISPR adaptation. Therefore, we propose that slipped spacers are most likely to confer a host advantage against phages that are very susceptible to CRISPR-Cas interference, such as where a single host spacer confers strong immunity and against phage populations that have high genetic diversity, where the chance of escape mutant selection is elevated.

DISCUSSION

Slipped spacers have been reported as anomalies of CRISPR adaptation in all characterized type I systems ([Swarts et al., 2012; Savitskaya et al., 2013; Richter et al., 2014; Shmakov et al., 2014; Staals et al., 2016; Li et al., 2017; Rao et al., 2017](#)),

but it was previously unknown whether they had any biological role. Here, we discovered that slipped spacers in two different type I systems and different bacteria are less effective for defense but enhance primed CRISPR adaptation. Since invader DNA is required to form substrates for CRISPR adaptation, our data support a trade-off between efficient defense and the opportunity to update immunity. Because canonical spacers typically facilitate rapid targeting and clearance of invading DNA, only a small amount of substrates are available for the acquisition of additional spacers. By contrast, slipped spacers provide less effective target recognition, thereby allowing more opportunity for target replication and consequently an increased abundance of potential spacer substrates. Previous modeling supports this correlation between the maximum copy number of invading DNA targets and the amount of CRISPR adaptation ([Severinov et al., 2016](#)). Overall, we propose a model where slipped spacers in type I CRISPR-Cas systems provide a pathway to priming that leads to increased CRISPR diversity, which results in a population-level advantage to hosts during coevolution with phages ([Figure 7](#)).

Our protospacer mapping data ([Figure 3G](#)) support that the mechanisms for priming with canonical and slipped spacers, and likely also for target mutants, are the same. This is further supported by *in vitro* and *in vivo* analyses of target protospacer recognition and priming in the *E. coli* type I-E system ([Krivoy et al., 2018](#)). The important distinction of priming by slipped spacers compared with priming from PAM and protospacer escape mutations is that slipping allows efficient priming in a sub-population of cells before escape mutants become prevalent. The resulting hyper-diversity of CRISPR loci in these subpopulations is likely to provide more resilient immunity across the population ([Childs et al., 2014; van Houte et al., 2016](#)). Moreover, since phage escape mutants that stimulate priming will be selected against during coevolution, it is more likely that viral sweeps will be driven by mutants that abrogate the hosts' priming response, such as recombination events that eliminate entire protospacers ([Paez-Espino et al., 2015](#)). We therefore propose that priming initiated by slipped spacers is a more robust pathway to increase CRISPR diversity compared to priming from escape mutants with canonical spacers. In support of this concept, previous modeling implies that during phage-host coevolution with only canonical spacers, increased rates of viral mutation result in less CRISPR diversity ([Martynov et al., 2017](#)).

Our slipping model for the generation of immune diversity to protect bacterial populations is supported by previous studies of primed CRISPR adaptation in *Pseudomonas aeruginosa* ([Westra et al., 2015; van Houte et al., 2016](#)), which possesses several spacers that imperfectly target the DMS3vir phage ([Cady et al., 2012; Heussler et al., 2016](#)). Due to the imperfect targeting (resulting from spacer-target mismatches and PAM mutations), phage-infected cells cannot immediately defend against DMS3vir. However, a small proportion of bacteria undergo priming, survive, and proliferate ([Cady et al., 2012; Westra et al., 2015](#)). Since many different spacers are acquired by the cells that undergo priming, the resulting population diversity of CRISPR loci provides robust immunity that limits the chance for phages to escape CRISPR immunity via mutation ([Levin et al., 2013; van Houte et al., 2016; Chabas et al., 2018](#)). This bust-and-boom phenomenon is analogous to our

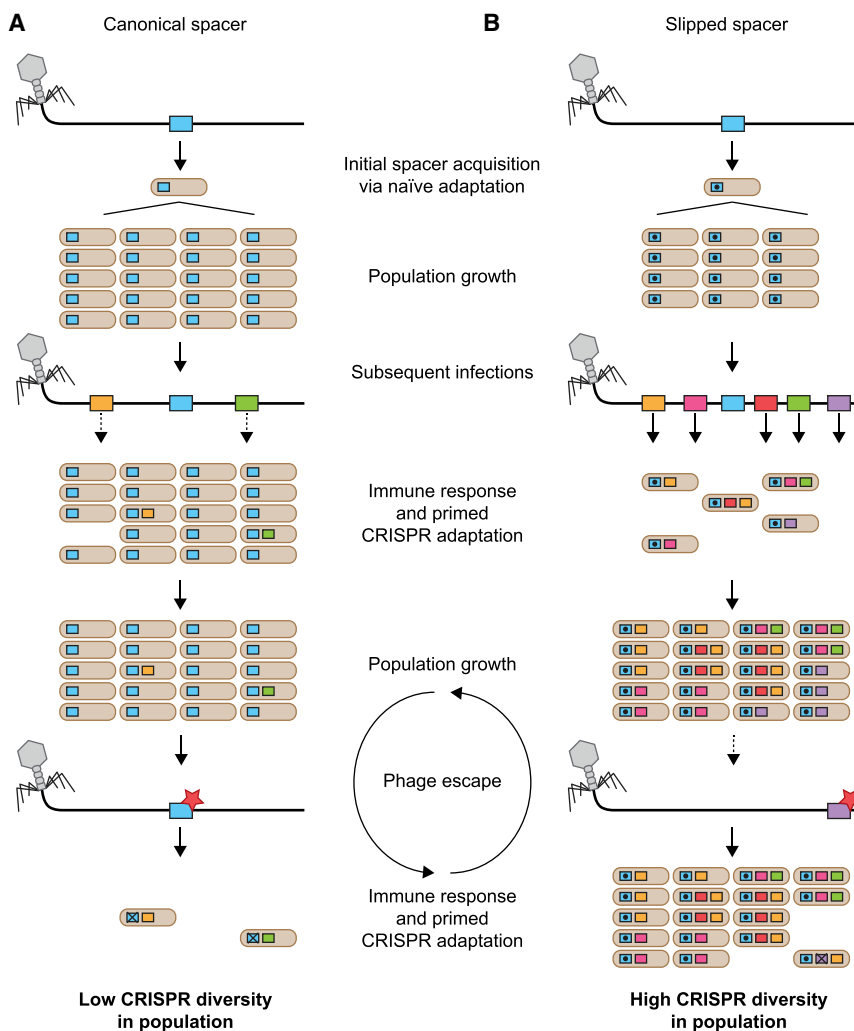


Figure 7. The Establishment of CRISPR Diversity Stimulated by Slipped Spacers

(A) In the absence of existing immunity, a canonical spacer (blue) can be acquired by naïve adaptation. The progeny of this cell will have clonal immunity. Upon reinfection with the WT phage, interference with the canonical spacer is efficient and only a small proportion of new cells acquire additional spacers. If a phage mutant arises that escapes the initial (blue) spacer, only the small proportion of cells that possess other spacers will have immunity. The outcome is a population with low CRISPR diversity and less resilience to an evolving phage population.

(B) If the initial spacer acquired by naïve CRISPR adaptation is a slipped spacer, the resulting clonal population is more susceptible to the WT phage; however, more of the infected cells acquire new spacers. The resulting population has high CRISPR diversity and is less susceptible to phage mutants. In the context of phage-host coevolution, the first spacer in (A) and (B) need not necessarily be acquired by naïve adaptation. The same pathways will occur in situations when a host initially possesses two spacers, either both canonical or one canonical and one slipped, and one canonical spacer is rendered obsolete via a substantial phage mutation, such as recombination eliminating the protospacer. Indeed, this impact in coevolving populations predominantly contributes to the benefits of slipping in our agent-based modeling (Figure 6).

proposed ecological role of slipped spacers (Figure 7). For all type I systems where subpopulations of cells possess slipped spacers, we propose that slipping represents a conserved “bet-hedging” strategy for CRISPR-Cas immunity that allows a proportion of hosts to potentially gain more spacers during infections, before phage escape mutants proliferate.

Slipped spacers have also been observed in type II CRISPR-Cas systems (Paez-Espino et al., 2013; Wei et al., 2015). Despite the absence of experimental data of primed CRISPR adaptation in type II systems, bioinformatics analyses support that it occurs (Nicholson et al., 2018). As such, we predict that slipped spacers in type II systems will provide a population-level advantage analogous to slipping in type I systems. Furthermore, we propose that the inverse correlation between efficient target clearance and the opportunity to generate substrates for spacer acquisition (Severinov et al., 2016) applies to any spacers that are less efficient for interference. For example, non-canonical PAM selection during spacer acquisition has been observed at levels comparable to slipping (e.g., type I-E systems also use CCT, CAT) and there is evidence that some of these stimulate priming (Yosef et al., 2012; Fineran et al., 2014; Shmakov et al., 2014; Xue et al., 2015). We propose

that these spacers play a biological role similar to that of slipped spacers by tempering interference and increasing priming. High viral mutation rates have previously been predicted to result in selection against the maintenance of

CRISPR-Cas immunity that acts in a reactionary manner, which raised the question of why pre-emptive CRISPR-Cas immune diversification has not evolved (Weinberger et al., 2012). We propose that imprecise spacer acquisition represents a form of immune bet-hedging that enables bacterial communities to pre-empt the proliferation of potential phage escape mutants that might otherwise render CRISPR-Cas defenses ineffective.

STAR METHODS

Detailed methods are provided in the online version of this paper and include the following:

- KEY RESOURCES TABLE
- CONTACT FOR REAGENT AND RESOURCE SHARING
- EXPERIMENTAL MODEL AND SUBJECT DETAILS
 - Bacterial and Virus strains
 - Mutant strain construction
- METHOD DETAILS
 - Interference assays
 - Plasmid loss assays
 - Iterative infection (pestering)

- High-throughput analyses of CRISPR expansion
- Phage EOP and infection time courses
- Agent-based modelling
- QUANTIFICATION AND STATISTICAL ANALYSIS
- DATA AND SOFTWARE AVAILABILITY

SUPPLEMENTAL INFORMATION

Supplemental Information includes six figures and six tables and can be found with this article online at <https://doi.org/10.1016/j.chom.2018.12.014>.

ACKNOWLEDGMENTS

We thank Corinda Taylor for assistance with generating transconjugants, Bridget Watson for providing *P. atrosepticum* strains used as controls for normalization of the pestered cell population NGS assay, and Keith Ireton for feedback on the manuscript. This research was funded by the Marsden Fund, Royal Society of New Zealand (RSNZ), and a Rutherford Discovery Fellowship (RSNZ) to P.C.F. N.B. and L.M.M. were funded by University of Otago Doctoral Scholarships. We also acknowledge the use of the New Zealand eScience Infrastructure (NeSI) high-performance computing facilities in this research. NeSI's facilities are provided by and funded jointly by NeSI's collaborator institutions and through the Ministry of Business, Innovation and Employment's Research Infrastructure programme.

AUTHOR CONTRIBUTIONS

S.A.J., N.B., L.M.M., and P.C.F. designed experiments. S.A.J., N.B., and L.M.M. performed the experiments. S.A.J., N.B., L.M.M., and P.C.F. analyzed the data. S.A.J. and P.C.F. wrote the manuscript with input from the other authors.

DECLARATION OF INTERESTS

The authors declare no competing interests.

Received: July 9, 2018

Revised: October 18, 2018

Accepted: December 14, 2018

Published: January 17, 2019

REFERENCES

- Amitai, G., and Sorek, R. (2016). CRISPR-Cas adaptation: insights into the mechanism of action. *Nat. Rev. Microbiol.* **14**, 67–76.
- Andersson, A.F., and Banfield, J.F. (2008). Virus population dynamics and acquired virus resistance in natural microbial communities. *Science* **320**, 1047–1050.
- Barrangou, R., Fremaux, C., Deveau, H., Richards, M., Boyaval, P., Moineau, S., Romero, D.A., and Horvath, P. (2007). CRISPR provides acquired resistance against viruses in prokaryotes. *Science* **315**, 1709–1712.
- Brouns, S.J., Jore, M.M., Lundgren, M., Westra, E.R., Slijkhuis, R.J., Snijders, A.P., Dickman, M.J., Makarova, K.S., Koonin, E.V., and van der Oost, J. (2008). Small crisper RNAs guide antiviral defense in prokaryotes. *Science* **321**, 960–964.
- Cady, K.C., Bondy-Denomy, J., Heussler, G.E., Davidson, A.R., and O'Toole, G.A. (2012). The CRISPR/Cas adaptive immune system of *Pseudomonas aeruginosa* mediates resistance to naturally occurring and engineered phages. *J. Bacteriol.* **194**, 5728–5738.
- Chabas, H., Lion, S., Nicot, A., Meaden, S., van Houte, S., Moineau, S., Wahl, L.M., Westra, E.R., and Gandon, S. (2018). Evolutionary emergence of infectious diseases in heterogeneous host populations. *PLoS Biol.* **16**, e2006738.
- Childs, L.M., England, W.E., Young, M.J., Weitz, J.S., and Whitaker, R.J. (2014). CRISPR-induced distributed immunity in microbial populations. *PLoS One* **9**, e101710.
- Datsenko, K.A., Pougach, K., Tikhonov, A., Wanner, B.L., Severinov, K., and Semenova, E. (2012). Molecular memory of prior infections activates the CRISPR/Cas adaptive bacterial immunity system. *Nat. Commun.* **3**, 945.
- Deveau, H., Barrangou, R., Garneau, J.E., Labonté, J., Fremaux, C., Boyaval, P., Romero, D.A., Horvath, P., and Moineau, S. (2008). Phage response to CRISPR-encoded resistance in *Streptococcus thermophilus*. *J. Bacteriol.* **190**, 1390–1400.
- Fagerlund, R.D., Wilkinson, M.E., Klykov, O., Barendregt, A., Pearce, F.G., Kieper, S.N., Maxwell, H.W.R., Capolupo, A., Heck, A.J.R., Krause, K.L., et al. (2017). Spacer capture and integration by a type I-F Cas1-Cas2-3 CRISPR adaptation complex. *Proc. Natl. Acad. Sci. USA* **114**, E5122–E5128.
- Fineran, P.C., Gerritzen, M.J., Suárez-Diez, M., Küne, T., Boekhorst, J., van Hijum, S.A., Staals, R.H., and Brouns, S.J. (2014). Degenerate target sites mediate rapid primed CRISPR adaptation. *Proc. Natl. Acad. Sci. USA* **111**, E1629–1638.
- Fineran, P.C., Iglesias Cans, M.C., Ramsay, J.P., Wilf, N.M., Cossyleon, D., McNeil, M.B., Williamson, N.R., Monson, R.E., Becher, S.A., Stanton, J.A., et al. (2013). Draft genome sequence of *Serratia* sp. Strain ATCC 39006, a model bacterium for analysis of the biosynthesis and regulation of prodigiosin, a carbapenem, and gas vesicles. *Genome Announc.* **1**, e01039–13.
- Haerter, J.O., and Sneppen, K. (2012). Spatial structure and Lamarckian adaptation explain extreme genetic diversity at CRISPR locus. *MBio* **3**, e00126–12.
- Haerter, J.O., Trusina, A., and Sneppen, K. (2011). Targeted bacterial immunity buffers phage diversity. *J. Virol.* **85**, 10554–10560.
- Heilmann, S., Sneppen, K., and Krishna, S. (2010). Sustainability of virulence in a phage-bacterial ecosystem. *J. Virol.* **84**, 3016–3022.
- Held, N.L., Herrera, A., Cadillo-Quiroz, H., and Whitaker, R.J. (2010). CRISPR associated diversity within a population of *Sulfolobus islandicus*. *PLoS One* **5**, e12988.
- Heussler, G.E., Miller, J.L., Price, C.E., Collins, A.J., and O'Toole, G.A. (2016). Requirements for *Pseudomonas aeruginosa* type I-F CRISPR-cas adaptation determined using a biofilm enrichment assay. *J. Bacteriol.* **198**, 3080–3090.
- Horvath, P., Romero, D.A., Coûté-Monvoisin, A.C., Richards, M., Deveau, H., Moineau, S., Boyaval, P., Fremaux, C., and Barrangou, R. (2008). Diversity, activity, and evolution of CRISPR loci in *Streptococcus thermophilus*. *J. Bacteriol.* **190**, 1401–1412.
- Iranzo, J., Lobkovsky, A.E., Wolf, Y.I., and Koonin, E.V. (2013). Evolutionary dynamics of the prokaryotic adaptive immunity system CRISPR-Cas in an explicit ecological context. *J. Bacteriol.* **195**, 3834–3844.
- Jackson, S.A., McKenzie, R.E., Fagerlund, R.D., Kieper, S.N., Fineran, P.C., and Brouns, S.J. (2017). CRISPR-Cas: adapting to change. *Science* **356**, eaal5056.
- Koonin, E.V., Makarova, K.S., and Zhang, F. (2017). Diversity, classification and evolution of CRISPR-Cas systems. *Curr. Opin. Microbiol.* **37**, 67–78.
- Krivoy, A., Rutkauskas, M., Kuznedelov, K., Musharova, O., Rouillon, C., Severinov, K., and Seidel, R. (2018). Primed CRISPR adaptation in *Escherichia coli* cells does not depend on conformational changes in the Cascade effector complex detected in vitro. *Nucleic Acids Res.* **46**, 4087–4098.
- Leenay, R.T., Maksimchuk, K.R., Slotkowski, R.A., Agrawal, R.N., Gomaa, A.A., Briner, A.E., Barrangou, R., and Beisel, C.L. (2016). Identifying and visualizing functional PAM diversity across CRISPR-cas systems. *Mol. Cell* **62**, 137–147.
- Levin, B.R., Moineau, S., Bushman, M., and Barrangou, R. (2013). The population and evolutionary dynamics of phage and bacteria with CRISPR-mediated immunity. *PLoS Genet.* **9**, e1003312.
- Li, M., Gong, L., Zhao, D., Zhou, J., and Xiang, H. (2017). The spacer size of I-B CRISPR is modulated by the terminal sequence of the protospacer. *Nucleic Acids Res.* **45**, 4642–4654.
- Makarova, K.S., Wolf, Y.I., Alkhnbashi, O.S., Costa, F., Shah, S.A., Saunders, S.J., Barrangou, R., Brouns, S.J., Charpentier, E., Haft, D.H., et al. (2015). An updated evolutionary classification of CRISPR-Cas systems. *Nat. Rev. Microbiol.* **13**, 722–736.

- Marraffini, L.A., and Sontheimer, E.J. (2008). CRISPR interference limits horizontal gene transfer in staphylococci by targeting DNA. *Science* 322, 1843–1845.
- Martynov, A., Severinov, K., and Ispolatov, I. (2017). Optimal number of spacers in CRISPR arrays. *PLoS Comput. Biol.* 13, e1005891.
- Mojica, F.J., Díez-Villaseñor, C., García-Martínez, J., and Almendros, C. (2009). Short motif sequences determine the targets of the prokaryotic CRISPR defence system. *Microbiology (Reading, Engl.)* 155, 733–740.
- Nicholson, T.J., Jackson, S.A., Croft, B.I., Staals, R.H.J., Fineran, P.C., and Brown, C.M. (2018). Bioinformatic evidence of widespread priming in type I and II CRISPR-Cas systems. *RNA Biol.* 1–11.
- Paez-Espino, D., Morovic, W., Sun, C.L., Thomas, B.C., Ueda, K., Stahl, B., Barrangou, R., and Banfield, J.F. (2013). Strong bias in the bacterial CRISPR elements that confer immunity to phage. *Nat. Commun.* 4, 1430.
- Paez-Espino, D., Sharon, I., Morovic, W., Stahl, B., Thomas, B.C., Barrangou, R., and Banfield, J.F. (2015). CRISPR immunity drives rapid phage genome evolution in *Streptococcus thermophilus*. *MBio* 6, <https://doi.org/10.1128/mBio.00262-15>.
- Patterson, A.G., Jackson, S.A., Taylor, C., Evans, G.B., Salmon, G.P.C., Przybilski, R., Staals, R.H.J., and Fineran, P.C. (2016). Quorum sensing controls adaptive immunity through the regulation of multiple CRISPR-cas systems. *Mol. Cell* 64, 1102–1108.
- Rao, C., Chin, D., and Ensminger, A.W. (2017). Priming in A permissive type I-C CRISPR-cas system reveals distinct dynamics of spacer acquisition and loss. *RNA* 23, 525–1538.
- Richter, C., Dy, R.L., McKenzie, R.E., Watson, B.N., Taylor, C., Chang, J.T., McNeil, M.B., Staals, R.H., and Fineran, P.C. (2014). Priming in the Type I-F CRISPR-Cas system triggers strand-independent spacer acquisition, bi-directionally from the primed protospacer. *Nucleic Acids Res.* 42, 8516–8526.
- Savitskaya, E., Semenova, E., Dedkov, V., Metlitskaya, A., and Severinov, K. (2013). High-throughput analysis of type I-E CRISPR/Cas spacer acquisition in *E. coli*. *RNA Biol.* 10, 716–725.
- Semenova, E., Jore, M.M., Datsenko, K.A., Semenova, A., Westra, E.R., Wanner, B., van der Oost, J., Brouns, S.J., and Severinov, K. (2011). Interference by clustered regularly interspaced short palindromic repeat (CRISPR) RNA is governed by a seed sequence. *Proc. Natl. Acad. Sci. USA* 108, 10098–10103.
- Semenova, E., Savitskaya, E., Musharova, O., Strotkskaya, A., Vorontsova, D., Datsenko, K.A., Logacheva, M.D., and Severinov, K. (2016). Highly efficient primed spacer acquisition from targets destroyed by the *Escherichia coli* type I-E CRISPR-Cas interfering complex. *Proc. Natl. Acad. Sci. USA* 113, 7626–7631.
- Severinov, K., Ispolatov, I., and Semenova, E. (2016). The influence of copy-number of targeted extrachromosomal genetic elements on the outcome of CRISPR-cas defense. *Front. Mol. Biosci.* 3, 45.
- Shmakov, S., Abudayyeh, O.O., Makarova, K.S., Wolf, Y.I., Gootenberg, J.S., Semenova, E., Minakhin, L., Joung, J., Konermann, S., Severinov, K., et al. (2015). Discovery and functional characterization of diverse Class 2 CRISPR-cas systems. *Mol. Cell* 60, 385–397.
- Shmakov, S., Savitskaya, E., Semenova, E., Logacheva, M.D., Datsenko, K.A., and Severinov, K. (2014). Pervasive generation of oppositely oriented spacers during CRISPR adaptation. *Nucleic Acids Res.* 42, 5907–5916.
- Staals, R.H., Jackson, S.A., Biswas, A., Brouns, S.J., Brown, C.M., and Fineran, P.C. (2016). Interference-driven spacer acquisition is dominant over naive and primed adaptation in a native CRISPR-Cas system. *Nat. Commun.* 7, 12853.
- Sternberg, S.H., Richter, H., Charpentier, E., and Qimron, U. (2016). Adaptation in CRISPR-cas systems. *Mol. Cell* 61, 797–808.
- Swarts, D.C., Mosterd, C., van Passel, M.W., and Brouns, S.J. (2012). CRISPR interference directs strand specific spacer acquisition. *PLoS One* 7, e35888.
- Thoma, S., and Schobert, M. (2009). An improved *Escherichia coli* donor strain for diparental mating. *FEMS Microbiol. Lett.* 294, 127–132.
- Thomson, N.R., Crow, M.A., McGowan, S.J., Cox, A., and Salmon, G.P. (2000). Biosynthesis of carbapenem antibiotic and prodigiosin pigment in *Serratia* is under quorum sensing control. *Mol. Microbiol.* 36, 539–556.
- van Houte, S., Ekroth, A.K., Broniewski, J.M., Chabas, H., Ashby, B., Bondy-Denomy, J., Gandon, S., Boots, M., Paterson, S., Buckling, A., et al. (2016). The diversity-generating benefits of a prokaryotic adaptive immune system. *Nature* 532, 385–388.
- Wei, Y., Terns, R.M., and Terns, M.P. (2015). Cas9 function and host genome sampling in Type II-A CRISPR-Cas adaptation. *Genes Dev.* 29, 356–361.
- Weinberger, A.D., Wolf, Y.I., Lobkovsky, A.E., Gilmore, M.S., and Koonin, E.V. (2012). Viral diversity threshold for adaptive immunity in prokaryotes. *MBio* 3, e00456–12.
- Weissman, J.L., Holmes, R., Barrangou, R., Moineau, S., Fagan, W.F., Levin, B., and Johnson, P.L.F. (2018). Immune loss as a driver of coexistence during host-phage coevolution. *ISME J.* 12, 585–597.
- Westra, E.R., Swarts, D.C., Staals, R.H., Jore, M.M., Brouns, S.J., and van der Oost, J. (2012). The CRISPRs, they are a-changin': how prokaryotes generate adaptive immunity. *Annu. Rev. Genet.* 46, 311–339.
- Westra, E.R., van Houte, S., Oyesiku-Blakemore, S., Makin, B., Broniewski, J.M., Best, A., Bondy-Denomy, J., Davidson, A., Boots, M., and Buckling, A. (2015). Parasite exposure drives selective evolution of constitutive versus inducible defense. *Curr. Biol.* 25, 1043–1049.
- Wilensky, U. (1999). NetLogo (Center for Connected Learning and Computer-Based Modeling, Northwestern University). <http://ccl.northwestern.edu/netlogo/>.
- Xue, C., Seetharam, A.S., Musharova, O., Severinov, K., Brouns, S.J., Severin, A.J., and Sashital, D.G. (2015). CRISPR interference and priming varies with individual spacer sequences. *Nucleic Acids Res.* 43, 10831–10847.
- Yosef, I., Goren, M.G., and Qimron, U. (2012). Proteins and DNA elements essential for the CRISPR adaptation process in *Escherichia coli*. *Nucleic Acids Res.* 40, 5569–5576.
- Zhang, J., Kobert, K., Flouri, T., and Stamatakis, A. (2014). PEAR: a fast and accurate Illumina Paired-End reAd mergeR. *Bioinformatics* 30, 614–620.

STAR★METHODS**KEY RESOURCES TABLE**

REAGENT or RESOURCE	SOURCE	IDENTIFIER
Bacterial and Virus Strains		
<i>Escherichia coli</i> ST18	Thoma and Schobert (2009)	N/A
<i>Pectobacterium atrosepticum</i> SCRI1043	ATCC	ATCC BAA-672
<i>Pectobacterium atrosepticum</i> SCRI1043 ΔCRISPR2/ΔCRISPR3 Km ^R	This study	PCF276
<i>Pectobacterium atrosepticum</i> SCRI1043 ΔCRISPR2/ΔCRISPR3	This study	PCF279
<i>Pectobacterium atrosepticum</i> SCRI1043 cas1, cas2-3 isogenic control strain for PCF284	This study	PCF280
<i>Pectobacterium atrosepticum</i> SCRI1043 Cas1 ^{D269A} mutant	This study	PCF284
<i>Serratia</i> sp. ATCC 39006 strain LacA	Thomson et al. (2000)	lac ⁻ EMS mutant, denoted WT
<i>Serratia</i> phage JS26	L.M.M. and P.C.F. (unpublished data)	N/A
Chemicals, Peptides, and Recombinant Proteins		
5-aminolevulinic acid hydrochloride (ALA)	ACROS ORGANICS	Cat#103920050
Kanamycin sulfate (Km)	Sigma-Aldrich	Cat#60615
Streptomycin sulfate (Sm)	Fluka	Cat#85880
Tetracycline hydrochloride (Tc)	Sigma-Aldrich	Cat#T3383
Critical Commercial Assays		
DNeasy Blood and Tissue kit	Qiagen	Cat#69506
MiSeq Reagent Kit v3 (600-cycle)	illumina	Cat#MS-102-3003
Deposited Data		
High-throughput sequencing data of CRISPR spacer acquisition	SRA	SRA:PRJNA506108
Experimental Models: Organisms/Strains		
Bacteria: <i>Pectobacterium atrosepticum</i> SCRI1043	ATCC	ATCC BAA-672
Bacteria: <i>Serratia</i> strain LacA	Thomson et al. (2000)	lac ⁻ EMS mutant of ATCC 39006
Oligonucleotides		
Primers	See Table S6 for primers	N/A
Recombinant DNA		
Plasmids	See Tables S2–S5 for plasmids	N/A
Software and Algorithms		
PEAR	Zhang et al. (2014)	http://www.exelixis-lab.org/web/software/pear
NetLogo v6.0	Wilensky (1999)	http://ccl.northwestern.edu/netlogo/

CONTACT FOR REAGENT AND RESOURCE SHARING

Further information and requests for resources and reagents should be directed to and will be fulfilled by the Lead Contact, Peter Fineran (peter.fineran@otago.ac.nz)

EXPERIMENTAL MODEL AND SUBJECT DETAILS**Bacterial and Virus strains**

P. atrosepticum and *Serratia* were grown in Lysogeny broth (LB) at 25°C and 30°C, respectively. The *E. coli* ST18 auxotrophic donor was grown at 37°C in LB supplemented with 5-aminolevulinic acid (ALA; 50 µg mL⁻¹). Liquid cultures for all bacteria were shaken at 180 rpm. All strains were stored at -80°C in 25% glycerol. Where appropriate, antibiotics were added to media at the following

concentrations: Kanamycin (Km ; 50 $\mu\text{g mL}^{-1}$), Streptomycin (Sm ; 50 $\mu\text{g mL}^{-1}$), and Tetracycline (Tc ; 10 $\mu\text{g mL}^{-1}$). JS26 is a recently isolated bacteriophage of the family *Siphoviridae* that infects *Serratia* sp. ATCC 39006 (L.M.M. and P.C.F., unpublished data). None of the endogenous *Serratia* sp. ATCC 39006 spacers align to the JS26 genome. JS26 was propagated on WT *Serratia* grown in LB at 30°C.

Mutant strain construction

To construct the Cas1^{D269A} point mutant, the region encompassing the *cas1* and most of *cas2-3* genes was first replaced, via allelic exchange mutagenesis using pPF1133, with a Sm^R resistance cassette. The entire *cas1* and *cas2-3* region was then reinserted using pPF1134 or pPF1138, to generate unmarked WT control (PCF280) and Cas1^{D269A} mutants (PCF284), respectively. A single array (CRISPR1) strain ((ΔCRISPR2/ΔCRISPR3, PCF279) was generated by allelic exchange mutagenesis using pPF891 to create a marked (Km^R) intermediate strain (PCF276), followed by pPF1128 to remove the Km^R cassette, leaving in place a T4 transcriptional terminator immediately after the *cas6f* stop codon.

METHOD DETAILS

Interference assays

Plasmid interference was determined using conjugation efficiency assays, as previously described (Richter et al., 2014; Patterson et al., 2016). Briefly, plasmids were conjugated from the *E. coli* donor ST18 into the *P. atrosepticum* or *Serratia* recipients by overnight mating (with a donor to recipient ratio of 1:1) on sterile mixed cellulose ester filters (0.22 μm , Millipore) placed on LB agar + ALA. The conjugation efficiency was determined by plating dilution series of the mating spots onto LB agar + Tc (transconjugants) and LB agar (total recipient count). The transconjugant frequency was defined as transconjugant CFU/recipient CFU.

Plasmid loss assays

For primed CRISPR adaptation assays the plasmids were conjugated from *E. coli* into *P. atrosepticum*, as above for the interference assays. The resulting transconjugants were grown overnight in 6 mL LB with antibiotics. Each culture was subsequently passaged for 5 days by the transfer of 6 μL of inoculum into 6 mL of fresh LB without antibiotics, according to Richter et al. (2014). To induce expression of a plasmid-borne fluorescent reporter (mCherry), under control of the T5/Lac promoter, all culture media were supplemented with 25 μM IPTG. The proportion of the cell population containing the plasmid was determined by flow cytometry using a BD LSRFortessa (561 nm laser, 610 \pm 20 nm bandpass filter).

Iterative infection (pestering)

The single array (CRISPR1) *P. atrosepticum* mutant (ΔCRISPR2/ΔCRISPR3), PCF279, was used as the recipient for the iterative infection assays. Plasmids were conjugated from *E. coli* ST18 into PCF279 by overnight mating/infection with a donor to recipient ratio of 50:1 on sterile mixed cellulose ester filters (0.22 μm , Millipore) placed on LB agar + ALA. The filters containing the mating spots were then transferred to 6 mL LB without antibiotics or ALA and grown with shaking for 8 - 10 h. These cultures were used to set up the second round of overnight mating/infection, with fresh *E. coli* donor cells, again placed on sterile filters on LB agar + ALA. The mating/infection and liquid growth cycles were repeated 4 times, followed by 3 cycles of donor outgrowth in LB (24 h each, with transfer of 12 μL inoculum into 6 mL fresh LB without antibiotic or ALA). To determine the average infection rate, dilution series from each daily mating/infection with the untargeted (no protospacer) plasmid were plated onto LB + 25 μM IPTG and the ratio of red (resulting from plasmid-borne mCherry expression) versus white colonies was determined by counting. For pestering assays with *Serratia*, a similar procedure was followed, with the following alterations: mating/infection spots were set up with a donor to recipient ratio of 5:1, mating/infection spots were incubated on plates for 20 - 22 h, the daily filter-inoculated cultures were grown for 22 - 24 h and a total of 3 infection cycles were performed. All pestering assays were performed in triplicate.

In the *P. atrosepticum* type I-F diversity analyses, we accounted for variations in sequencing depth by randomly sampling 100,000 CRISPR loci from each underlying population. To reduce inflation of the apparent richness by infrequently acquired non-canonical spacers, only 32 nt spacers mapping to GG PAMs are included in the analyses. Similarly, for the *Serratia* type I-E system, we sampled 20,000 CRISPR loci from each underlying population and considered only 32 nt spacers mapping to CTT PAMs.

High-throughput analyses of CRISPR expansion

To facilitate the assessment of CRISPR expansion in pestered host populations, as above, unbiased by PCR or staining efficiencies, we developed a quantitative high-throughput sequencing assay. The assay is based on PCR-derived amplicon sequencing and included internal controls to account for amplicon-size-induced biases in both PCR and sequencing efficiency, and to allow quantitative normalisation between samples. We used a 2-step PCR approach to generate amplicons pre-labelled with indexes and Illumina sequencing adapters. Genomic DNA (gDNA) was prepared from all pestered cell populations using a DNeasy Blood and Tissue kit (Qiagen). To enable quantitation of CRISPR expansion, we spiked in an internal control to each sample – consisting of gDNA prepared from hosts with +1 expanded CRISPRs containing unique phage-targeting spacers (these spacers do not match the pestering plasmid sequences). The first-round PCRs used locus-specific primer pairs for each of the triplicate samples (Table S6). The

second-round PCRs added indexes, to differentiate between samples, and sequencing adapters. For the CRISPR-size control samples, we performed the same 2-step amplification approach with triplicate samples consisting of equimolar amounts of gDNA from *P. atrosepticum* strains expanded by +0, +1, +2, +3, +4, +5 and +6 spacers in the CRISPR1 array. The pooled amplicon library was sequenced using a MiSeq v3 kit, with asymmetric paired-end reads (265 bp forward and 275 bp reverse). The reads were merged using PEAR (Zhang et al., 2014). The read lengths allowed arrays with up to 5 new spacers to be reliably merged. A series of R scripts was developed to de-multiplex reads, for quality control, to identify repeat and spacer sequences, and to map these to protospacers in the plasmids. To allow absolute quantitation on a per-cell basis, the data were normalised to the internal +1 CRISPR standard and corrected to account for amplicon-size biases (Figure S3A).

Phage EOP and infection time courses

Serratia strains possessing mini-CRISPR-containing plasmids were grown overnight in LB + Km + 0.1 mM IPTG. Efficiency of plaquing (EOP) assays were performed using 0.35% LB agar overlaid onto LB agar + Km + 0.1 mM IPTG. Non-specific controls expressed spacers that did not target the JS26 phage, with repeats from either the *Serratia* type I-E or type I-F systems, as appropriate. Time course infection assays were performed in 96-well plates using a multi-mode shaking plater reader (Varioskan, Thermo Scientific) at 30°C. The time courses were begun with cells at an OD₆₀₀ of 0.05 and a MOI of 0.01.

Agent-based modelling

To allow interrogation of the influence of slipped spacers within a simplistic host-phage infection system, we developed a stochastic agent-based model (ABM), which is based on previous studies that simulated host-phage interactions in spatially structured systems (Heilmann et al., 2010; Haerter et al., 2011; Haerter and Sneppen, 2012) and theoretical models of CRISPR-Cas activity and the assumptions and parameter estimates therein (Weinberger et al., 2012; Iranzo et al., 2013; Childs et al., 2014; Weissman et al., 2018). Briefly, our ABM consists of hosts that possess CRISPR-Cas systems and phages that are susceptible to CRISPR-Cas immunity. Hosts and phages are contained within a 100 x 100 square grid, which includes connectivity between opposing edges. Phages possess protospacer sites, which can be either WT or escape alleles. Host CRISPR-Cas systems can acquire spacers from protospacers within phage genomes. Spacers can be either canonical or slipped, with differing functional outcomes that are based on our experimental data. The parameters of the model are summarised in Table S1. Trials are initiated (as below) and run until either hosts or phages become extinct. The model is implemented in NetLogo v6.0 (Wilensky, 1999).

Initialisation: the grid is randomly populated with 90 naive hosts and 10 hosts each with one randomly selected spacer that targets the WT phage, and the host growth stages are randomised. The bacterial population is grown for 100 time steps (τ), which is sufficient for the hosts to reach approximately 50% of the maximum population density, then 50 phages are placed randomly in the model. The model then continues to progress in time steps until either phages or host are driven to extinction. At each step there are 4 main stages – *bacterial growth*, *phage infection*, *progression of infections*, and *phage decay and diffusion* – plus a *CRISPR adaptation* sub-stage, which are defined as follows:

Bacterial growth; non-infected cells with an unoccupied (by hosts) orthogonal space increase in growth stage. If the host growth stage reaches the doubling time then a new host, with identical genotype, is created on an adjacent empty space, and the growth stage of both hosts is reset. If there are no empty adjacent spaces, the host does not replicate until space becomes available.

Phage infection; a proportion of all phages equal to the adsorption rate ($P_{\text{Adsorption}}$) attempt to infect any hosts resident in the phage's grid space. If the host is already infected, then the phage adsorbs without influencing the existing infection and is removed from the system. If the host is not infected and does not possess any CRISPR spacers that target any of the phage's WT protospacers, then the host either becomes infected with the corresponding phage genotype, or potentially undergoes naive CRISPR adaptation ($P_{\text{Naive_Adaptation}}$); note that naive CRISPR adaptation was not incorporated in the main model, it is included as a control in the supplementary data. If the host possesses at least one canonical spacer that targets any one of the phage's WT protospacer alleles, then the infection is successfully cleared by CRISPR-Cas immunity and the phage is removed. During successful phage defence, there is a chance that the host gains an additional spacer via primed CRISPR adaptation during interference ($P_{\text{Interference_Adaptation}}$). If the infected host does not possess any canonical immunity, but possesses at least one slipped spacer that targets any one of the phage's WT protospacer alleles, then the host either becomes infected with the phage (with a probability of $1 - P_{\text{Slipped_Adaptation}}$) (ultimately resulting in lysis) or undergoes primed CRISPR adaptation then clears the infection ($P_{\text{Slipped_Adaptation}}$). During slipping-stimulated priming there is a chance that the host acquires two spacers ($P_{\text{Slipped_Multiple_Spacers}}$).

Progression of infections; the infection state of infected hosts is increased by 1. If a host's infection state reaches the burst time, new phages are generated and released onto randomly allocated adjacent grid spaces. Phages inherit the genotype of the original infecting phage, but with a chance ($P_{\text{Phage_Mutation}}$) that one of their protospacers acquires a mutation that prevents targeting by either canonical or slipped spacers, i.e. the allele becomes 'escape'. Phage escape mutations are independent of CRISPR-Cas activity, i.e. they arise stochastically during phage replication.

Phage decay and diffusion; a proportion of all phages ($P_{\text{Phage_Decay}}$) are removed from the model, then a proportion of all phages ($P_{\text{Phage_Movement}}$) are moved to a randomly selected orthogonally or diagonally adjacent square.

CRISPR adaptation; hosts acquire a new spacer that is distinct from those already possessed. The spacers are randomly selected from the available phage protospacers and are either canonical or slipped spacers (the probability of a slipped spacer = P_{Slip}). Each host CRISPR array can store up to 5 spacers, which are added on a first-in-first-out basis. Hosts that undergo CRISPR adaptation clear any current infection.

QUANTIFICATION AND STATISTICAL ANALYSIS

As indicated in the figure legends, all figures plot the mean and error bars represent the standard error of the mean (S.E.M.).

DATA AND SOFTWARE AVAILABILITY

The accession number for DNA sequencing data is SRA: PRJNA506108.

Supplemental Information

Imprecise Spacer Acquisition

**Generates CRISPR-Cas Immune Diversity
through Primed Adaptation**

Simon A. Jackson, Nils Birkholz, Lucía M. Malone, and Peter C. Fineran

Supplementary Figures

Imprecise spacer acquisition generates CRISPR-Cas immune diversity through primed adaptation

Simon A. Jackson*, Nils Birkholz, Lucía M. Malone, Peter C. Fineran*[†]

Cell Host & Microbe

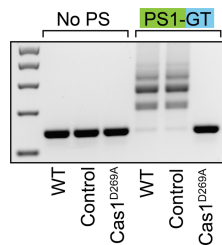


Figure S1: The Cas1^{D269A} *P. atrosepticum* strain is deficient in primed CRISPR adaptation; relates to Figure 2. Transconjugants possessing plasmids containing either no protospacer (no PS) or a priming protospacer matching spacer 1 with a GT PAM (PS1-GT) were passaged for 5 days and CRISPR adaptation was assessed by PCR of the CRISPR1 array, as per the Methods. The control strain is a mutagenesis control where the WT *cas1,cas2-3* operon was reinserted into the intermediate deletion strain in the original genomic context, whereas for the Cas1^{D269A} strain the mutated operon was inserted in the same location.

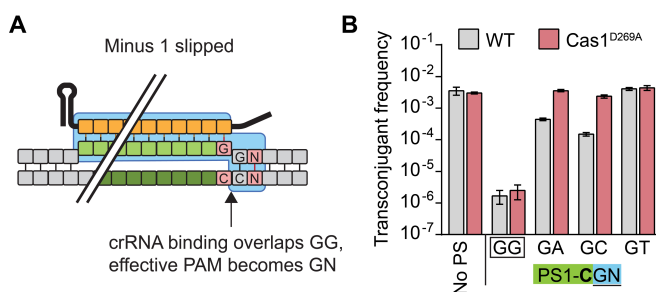


Figure S2: Minus 1 slips may result in GN PAMs; relates to Figure 2. **A)** Schematic of the PAM-sensing and crRNA binding sequence determinants (outlined in blue) proposed for target recognition with -1 slipped spacers; in this model, we predict that the nucleotide in position [1] of the crRNA (i.e. C) pairs with the first G of the canonical PAM. **B)** Plasmid interference data for GN PAM mutant targets of spacer 1. Data shown are the mean \pm SEM ($n \geq 3$).

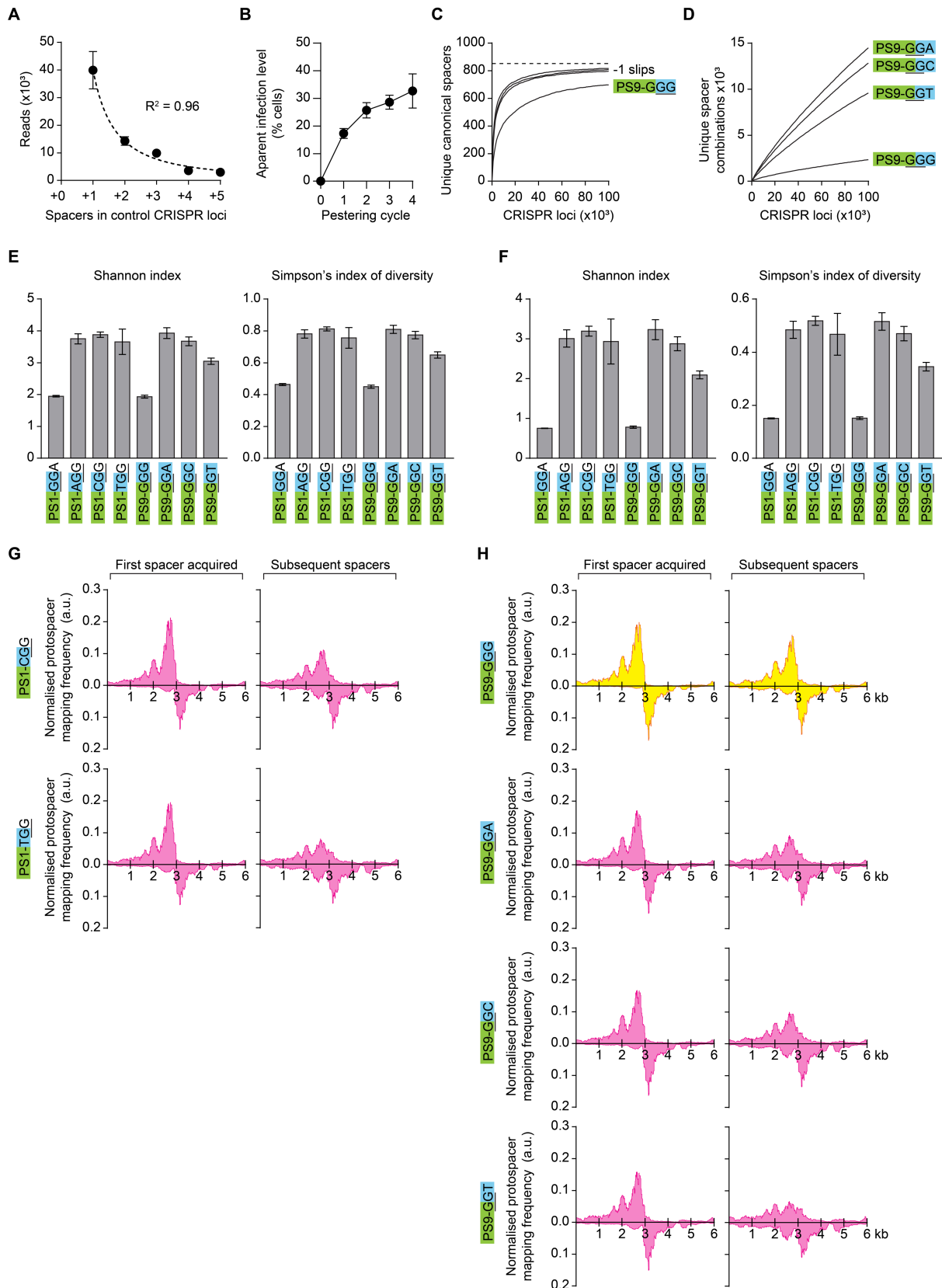


Figure S3: Quantitation of type I-F CRISPR diversity in pestered cell populations; relates to Figure 3. A) Detection biases for quantitation of CRISPR expansion by deep sequencing. Genomic DNA from strains with CRISPRs expanded by +0 to +5 spacers were combined in control samples ($n = 3$). In the absence of PCR, gel extraction, sequencing or analysis biases,

an equal number of reads is expected for the +1 to +6 control CRISPRs (the +0 CRISPRs were depleted by gel extraction). The dashed line represents the best-fit exponential. **B)** The apparent infection rate for the *P. atrosepticum* samples pestered with the no PS control plasmid, determined by plating and screening for the plasmid-borne fluorescent reporter (mCherry). **C)** Canonical plasmid-targeting spacer richness for pestered cell populations. The dashed line represents the maximum potential of unique canonical spacers, based on the plasmid sequence. **D)** Unique spacer combinations, irrespective of their order within arrays. To reduce artificial inflation, unique spacer combinations, rather than permutations, were calculated. **E)** Spacer diversity indices, based on the data in (C) and **Figure 3D**. **F)** CRISPR loci diversity indices, based on the data in (D) and **Figure 3E**. **G)** Additional protospacer mapping plots for PS1 samples shown in **Figure 3G**, normalised to the total number of protospacers displayed in each sample and separated into the first acquired spacers and subsequent spacers. The data are smoothed by rolling-sum windows of 250 bp, resulting in an arbitrary density scale. Protospacers mapped to the non-target strand are graphed above the x-axes, whereas those mapping to the target strand (i.e. containing the target protospacer sequence) are graphed below the axes. **H)** Protospacer mapping plots as in (G), for PS9 samples. Data in A, B, E and F are the mean \pm SEM ($n = 3$) and C, D, G and H are the mean ($n = 3$).

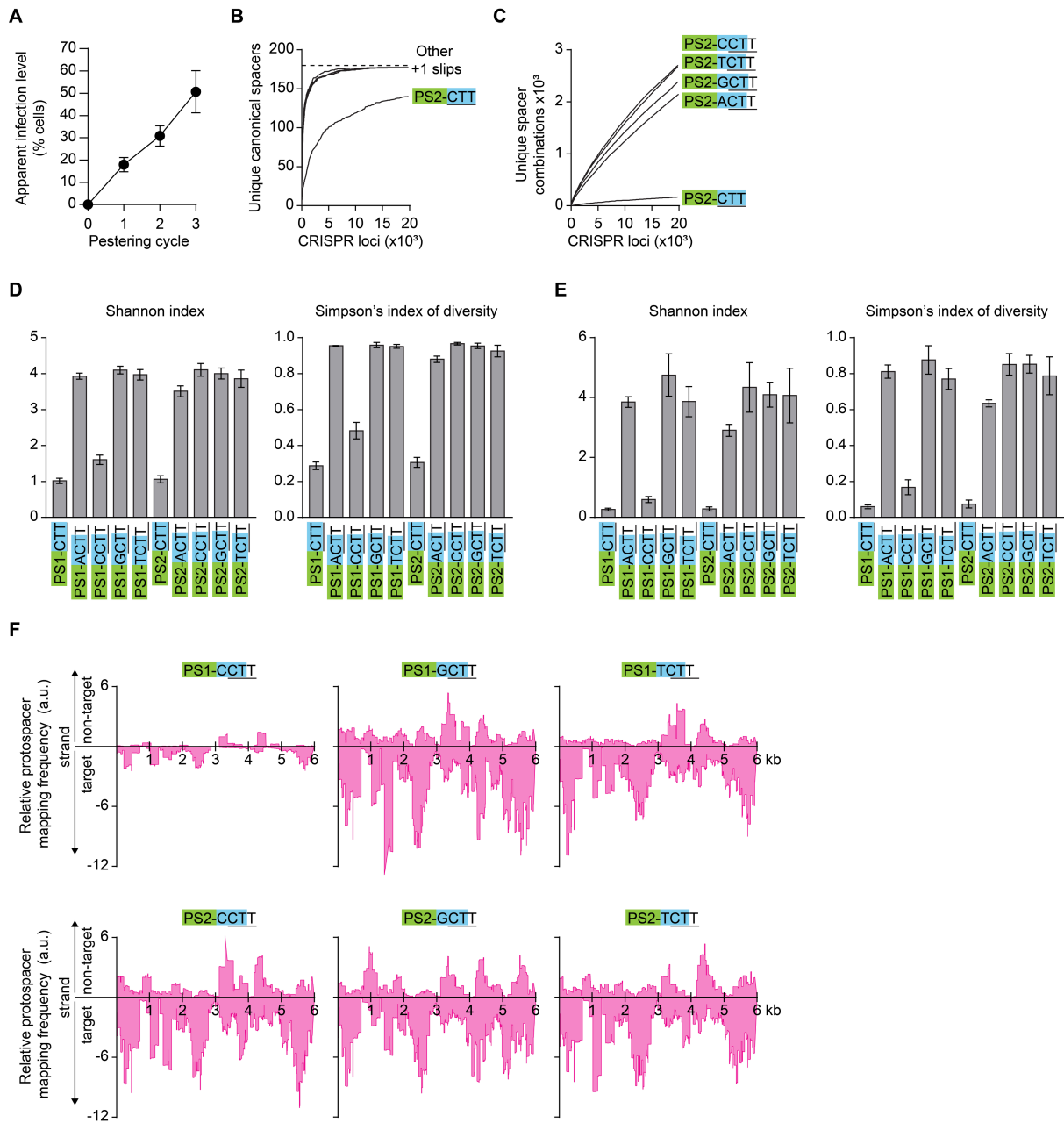


Figure S4: Quantitation of type I-E CRISPR diversity in pestered cell populations; related to Figure 4. **A)** The apparent infection rate for the *Serratia* samples pestered with untargeted (no protospacer) plasmids, determined by plating and screening for the plasmid-borne fluorescent reporter (mCherry). **B)** Canonical plasmid-targeting spacer richness for pestered cell populations. The dashed line represents the maximum potential of unique canonical spacers, based on the plasmid sequence. **C)** Unique spacer combinations, irrespective of their order within arrays. To reduce artificial inflation, unique spacer combinations, rather than permutations, were calculated. **D)** Spacer diversity indices, based on the data in (B) and **Figure 4F**. **E)** CRISPR loci diversity indices, based on the data in (C) and **Figure 4G**. **F)** Mapping the source of new spacers (i.e. protospacer locations) for additional plasmids related to **Figure 4H**. The data are smoothed by rolling-sum windows of 250 bp. Protospacers mapped to the non-target strand are graphed above the x-axes, whereas those mapping to the target strand are graphed below the axes. Data in A, D and E are the mean \pm SEM ($n = 3$) and B, C and F are the mean ($n = 3$).

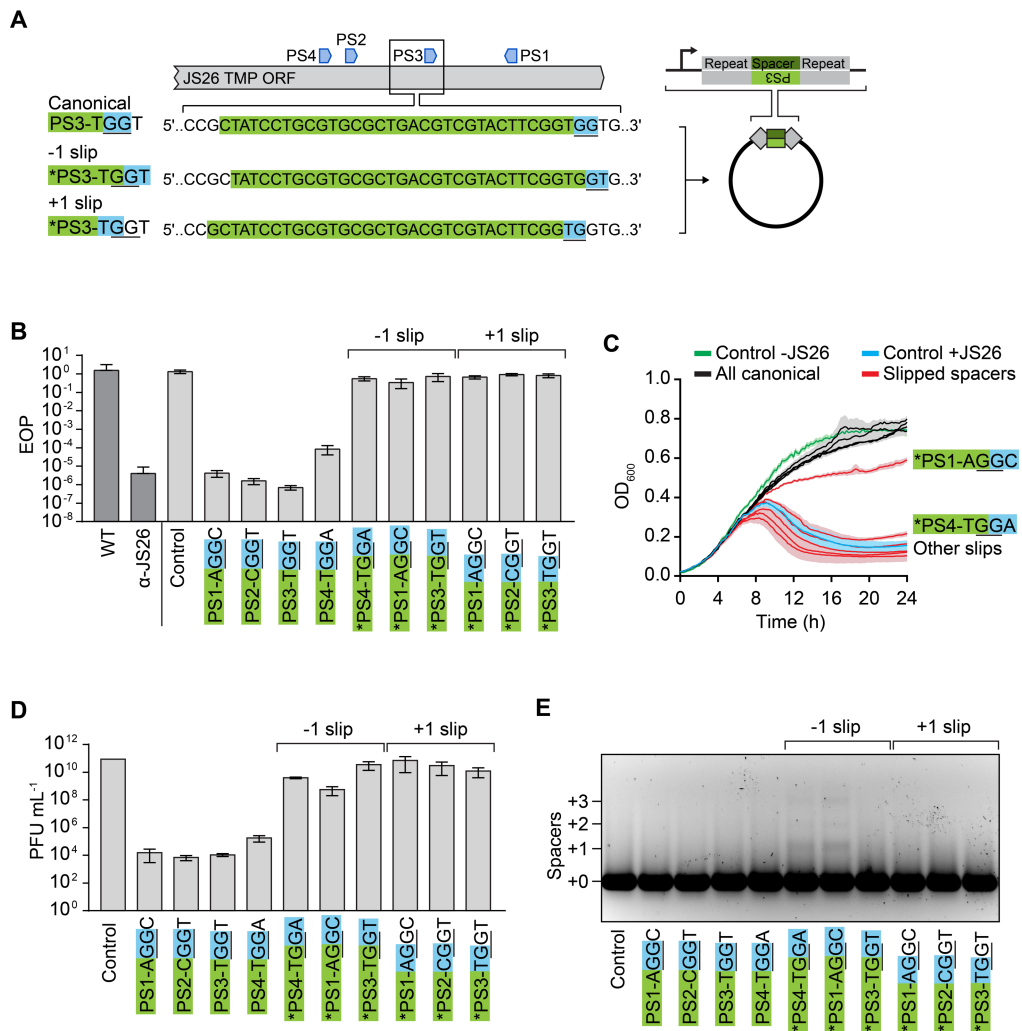


Figure S5: Slipped type I-F spacers increase CRISPR diversity during phage infection; relates to Figure 5. **A)** Schematic of the plasmid-borne mini-CRISPR locus harbouring canonical or slipped spacers for the *Serratia* type I-F system. The spacers target JS26 within the tape measure protein (TMP) coding region. **B)** Phage defence provided by canonical and slipped spacers, measured as the EOP relative to a negative control spacer that does not target JS26. WT *Serratia* and a bacteriophage-insensitive mutant that possesses a canonical spacer in the native type I-F CRISPR locus (α -JS26) are shown for comparison to the plasmid-borne mini-CRISPR strains. **C)** Time courses of growth in populations infected with JS26; MOI = 0.01. The shaded area bounding each line shows the SEM. **D)** Phage titres in infected populations (C) at the 24 h endpoint. **E)** CRISPR adaptation in infected populations (C) at the 24 h endpoint. Data shown are the mean \pm SEM ($n \geq 3$).

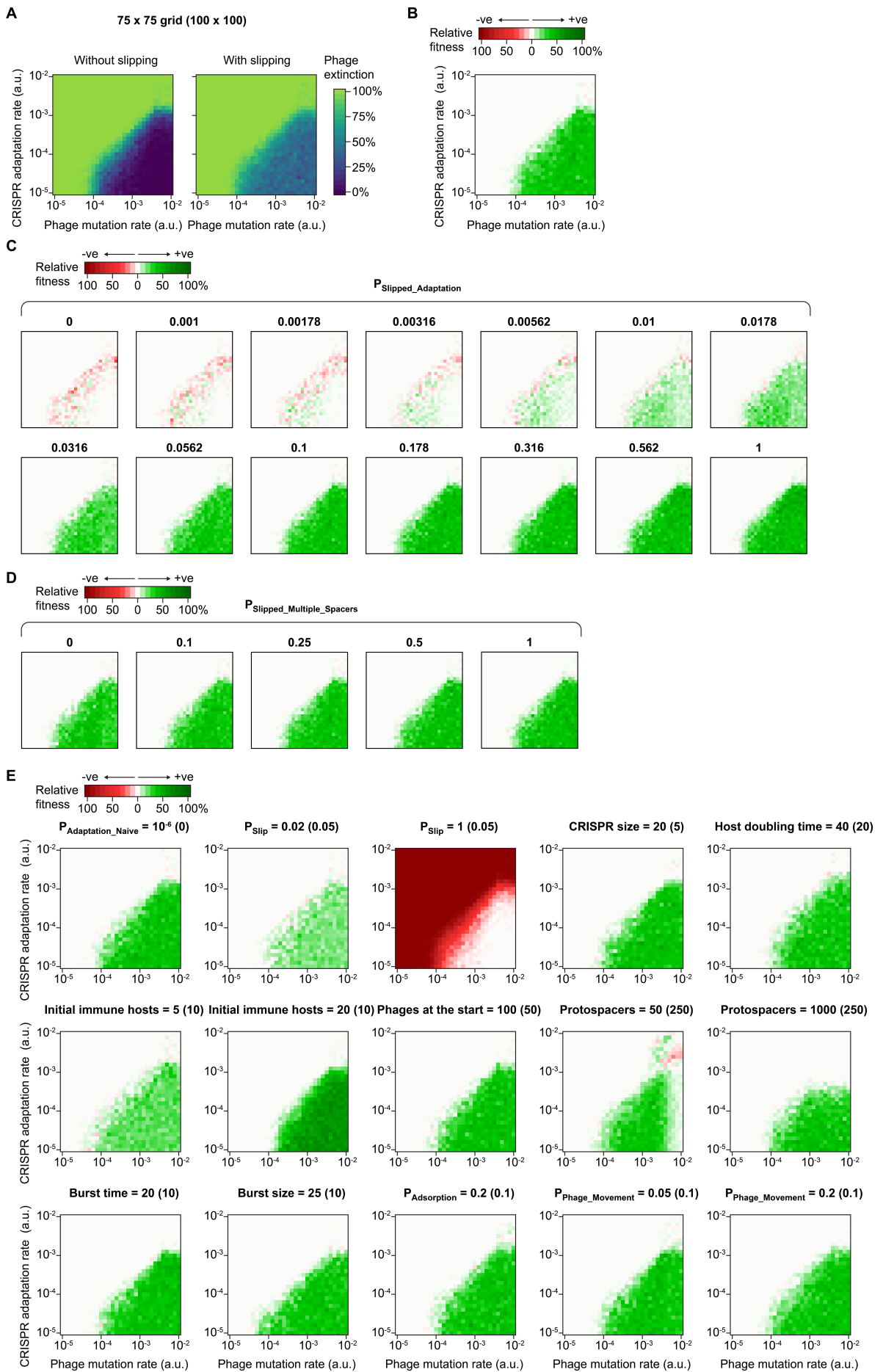


Figure S6: Additional modelling data obtained with varied parameters; relates to Figure 6. To reduce the computation time, a grid size of 75 x 75 (100 x 100 in **Figure 6**) was used for these simulations. **A)** Phage extinction using the 75 x 75 grid for comparison to **Figure 6C**. **B)** The relative fitness between populations with and without slipping (5%), measured as the difference in phage extinction outcomes as in (A). **C)** Variation of the ‘function’ of slipped spacers. In this case, the probability that an infected host relying on a slipped spacer undergoes CRISPR adaptation and survives was varied. These data were used to generate **Figure 6J**. **D)** Variation of the ‘function’ of slipped spacers, in this case the probability that slipped priming will result in the acquisition of two new spacers was varied (otherwise just one new spacer is acquired). **E)** Variation of additional agent-based model parameters. The parameters varied are labelled above each plot, with the values used in the main modelling analyses (**Figure 6**) given in parentheses. All data points represent 100 repetitions using a grid size of 75 x 75.

Table S1: Parameters for the agent-based modelling; relates to Figure 6.

Description [#]	Parameter	Value(s)*
Grid size		100 x 100
Time step	τ	Relative
Naïve hosts at the start		90 (95, 80)
Immune hosts at the start (each possesses one randomly acquired spacer)		10 (5, 20)
Phages added at $\tau = 100$		50 (100)
Host doubling time		20 τ (40)
Phage protospacers		250 (50, 1000)
Maximum spacers per CRISPR		5 (20)
Burst time		10 τ (20)
Burst size		10 (25)
Phage diffusion rate	$P_{\text{Phage_Movement}}$	0.1 τ (0.05, 0.2)
Phage decay rate	$P_{\text{Phage_Decay}}$	$10^{-3} \tau$
Phage adsorption rate	$P_{\text{Adsorption}}$	0.1 τ (0.2)
Phage mutation rate	$P_{\text{Phage_Mutation}}$	10^{-5} to 10^{-2}
Probability of naïve CRISPR adaptation	P_{Naive}	0 (10^{-6})
Probability of CRISPR adaptation during interference	$P_{\text{Interference_Adaptation}}$	10^{-5} to 10^{-2}
Slipping frequency	P_{Slip}	0 or 0.05 (0.02, 1)
Probability of priming by slipped spacers**/***	$P_{\text{Slipped_Adaptation}}$	0.1
Probability to acquire two spacers by slipping-stimulated priming	$P_{\text{Slipped_Multiple_Spacers}}$	0.1 (0, 0.25, 0.5, 1)

[#]Additional descriptions of these parameters are provided in the Methods.

*The specified values are for the main model (**Figure 6**) and the values in parentheses were tested using a grid size of 75 x 75 (**Figure S6**).

**Only used active in the absence of canonical immunity, i.e. if the host possesses any canonical spacers targeting WT phage protospacers, then any slipped spacers possessed by the host have no effect.

*** When priming does not occur ($1 - P_{\text{Slipped_Adaptation}}$), the infection is productive and leads to cell lysis and phage release, i.e. slipped spacers are always a trade-off between immunity and CRISPR adaptation.

Table S2: Bacterial strains; related to Figures 2-5.

Species	Strain	Description	Notes	Plasmid for construction	Reference
<i>E. coli</i>	DH5 α	Cloning strain			Gibco/BRL
<i>E. coli</i>	ST18	Auxotrophic donor for biparental conjugation	Requires ALA		Thoma and Schobert, 2009
<i>P. atrosepticum</i>	SCRI1043				
<i>P. atrosepticum</i>	PCF276	Δ CRISPR2/ Δ CRISPR3	Km ^R	pPF891	This study
<i>P. atrosepticum</i>	PCF278	Δ cas1:cas2-3	Sm ^R	pPF1133	This study
<i>P. atrosepticum</i>	PCF279	Δ CRISPR2/ Δ CRISPR3	Markerless	pPF1128	This study
<i>P. atrosepticum</i>	PCF280	Cas1:Cas2-3 mutagenesis WT control	Markerless	pPF1134	This study
<i>P. atrosepticum</i>	PCF284	Cas1:Cas2-3 mutagenesis Cas1 ^{D269A}	Markerless	pPF1138	This study
<i>Serratia</i> sp. ATCC 39006	LacA	<i>lac</i> ⁻ EMS mutant, denoted WT			Thomson <i>et al.</i> , 2000

Table S3: Plasmids for cloning and mutagenesis; relates to Figures 2-5.

Name	Features	Description	Construction	Reference
Construction of the ACRISPR2/ACRISPR3 and Cas1^{D269A} strains:				
pGEM-t-easy	Ap ^R	Cloning vector		Promega
pKNG101	R6K, OriT, sacB, SmR/SpR	Suicide vector for allelic exchange mutagenesis		Kaniga <i>et al.</i> , 1991
pPF923	Cm ^R , R6K, OriT, sacB	Suicide vector for allelic exchange mutagenesis	PF213/PF676 + PF1886/PF1918 (SalI/XbaI)	This study
pPF1117	Cm ^R , R6K, OriT, sacB	Suicide vector for allelic exchange mutagenesis	pPF923 PstI self-ligation	This study
pPF1131	Cm ^R , R6K, OriT, sacB	Suicide vector for allelic exchange mutagenesis	PF2189/PF2190 into pPF1117 (NheI/SacI)	This study
pPF891	Cm ^R , Km ^R , R6K, OriT, sacB	CRISPR2/3 Knockout Km ^R marked	PF1868/PF1869 + PF1913/PF1657 + PF1870/PF1871 (BamHI/XbaI into pKNG101)	This study
pPF1128	Cm ^R , R6K, OriT, sacB	CRISPR2/3 Knockout <i>csy4</i> ::T4term markerless	PF1868/PF2052 + PF2053/PF1871 (into pGEM-t-easy then BamHI/SphI into pPF1117)	This study
pPF700	Ap ^R	Cas1,Cas2-3 expression construct		Fagerlund <i>et al.</i> , 2017
pPF739	Ap ^R	Cas1 ^{D269A} ,Cas2-3 expression construct		Fagerlund <i>et al.</i> , 2017
pPF1132	Ap ^R , Sm ^R /Sp ^R	<i>cas1,cas2-3</i> Knockout pre-construct non-suicide	PF2191/PF2192 into pPF700 (KpnI/SphI)	This study
pPF1133	Cm ^R , R6K, OriT, sacB, Sm ^R /Sp ^R	<i>cas1,cas2-3</i> Knockout Sm ^R /Sp ^R marked	pPF1132 EcoRI/NheI(partial) into pPF1131 (MfeI/NheI)	This study
pPF1134	Cm ^R , R6K, OriT, sacB	<i>cas1,cas2-3</i> mutagenesis WT control	pPF700 EcoRI/NheI into pPF1131 (MfeI/NheI)	This study
pPF1138	Cm ^R , R6K, OriT, sacB	<i>cas1,cas2-3</i> mutagenesis Cas1 ^{D269A}	pPF739 EcoRI/NheI into pPF1131 (MfeI/NheI)	This study
Construction of plasmids expressing miniCRISPRs:				
pPF260	Km ^R , OriT, P _{T5/Lac}	General expression plasmid		Richter <i>et al.</i> , 2014
pPF974	Km ^R , OriT	mini-CRISPR base; Type I-E Repeat-BsaI-BsaI-Repeat	PF1962/PF1963 (EcoRI/SphI) into pPF260	This study
pPF975	Km ^R , OriT	mini-CRISPR base; Type I-F Repeat-BsaI-BsaI-Repeat	PF1964/PF1965 (EcoRI/SphI) into pPF260	This study
pPF1328	Km ^R , Tc ^R , OriT	mini-CRISPR base; Type I-E Repeat-BsaI-BsaI-Repeat	PF2527/PF2528 (XbaI) into pPF974 (NheI/XbaI)	This study
pPF1329	Km ^R , Tc ^R , OriT	mini-CRISPR base; Type I-F Repeat-BsaI-BsaI-Repeat	PF2527/PF2528 (XbaI) into pPF975 (NheI/XbaI)	This study

Table S4: Plasmids for interference, priming and pestering assays; related to Figures 2-4.

Name	Features	Host	System	Protospacer	PAM	Description	Specific primer*	Reference
pPF953	mCherry, Tc ^R , OriT		Untargeted control - lacks any protospacer	No PS			PF1615	This study
pPF954	mCherry, Tc ^R , OriT	<i>P. atrosepticum</i>	Type I-F	PS1	GGA	Canonical target	PF1955	This study
pPF998	mCherry, Tc ^R , OriT	<i>P. atrosepticum</i>	Type I-F	PS1	AGG	Slipping proxy (+1 slip)	PF2014	This study
pPF1053	mCherry, Tc ^R , OriT	<i>P. atrosepticum</i>	Type I-F	PS1	CGG	Slipping proxy (+1 slip)	PF2103	This study
pPF1054	mCherry, Tc ^R , OriT	<i>P. atrosepticum</i>	Type I-F	PS1	TGG	Slipping proxy (+1 slip)	PF2104	This study
pPF959	mCherry, Tc ^R , OriT	<i>P. atrosepticum</i>	Type I-F	PS1	AGA	PAM mutant	PF1968	This study
pPF963	mCherry, Tc ^R , OriT	<i>P. atrosepticum</i>	Type I-F	PS1	CGA	PAM mutant	PF1972	This study
pPF956	mCherry, Tc ^R , OriT	<i>P. atrosepticum</i>	Type I-F	PS1	TGA	PAM mutant	PF1957	This study
pPF967	mCherry, Tc ^R , OriT	<i>P. atrosepticum</i>	Type I-F	PS1	GTA	PAM mutant	PF1976	This study
pPF1201	mCherry, Tc ^R , OriT	<i>P. atrosepticum</i>	Type I-F	PS4	GGA	Canonical target	PF2264	This study
pPF1264	mCherry, Tc ^R , OriT	<i>P. atrosepticum</i>	Type I-F	PS4	GAA	Slipping proxy (-1 slip)	PF2408	This study
pPF1265	mCherry, Tc ^R , OriT	<i>P. atrosepticum</i>	Type I-F	PS4	GCA	Slipping proxy (-1 slip)	PF2409	This study
pPF1062	mCherry, Tc ^R , OriT	<i>P. atrosepticum</i>	Type I-F	PS4	GTA	Slipping proxy (-1 slip)	PF2120	This study
pPF1204	mCherry, Tc ^R , OriT	<i>P. atrosepticum</i>	Type I-F	PS9	GGA	Canonical target	PF2268	This study
pPF1268	mCherry, Tc ^R , OriT	<i>P. atrosepticum</i>	Type I-F	PS9	GAA	Slipping proxy (-1 slip)	PF2412	This study
pPF1269	mCherry, Tc ^R , OriT	<i>P. atrosepticum</i>	Type I-F	PS9	GCA	Slipping proxy (-1 slip)	PF2413	This study
pPF1065	mCherry, Tc ^R , OriT	<i>P. atrosepticum</i>	Type I-F	PS9	GTA	Slipping proxy (-1 slip)	PF2124	This study
pPF1203	mCherry, Tc ^R , OriT	<i>P. atrosepticum</i>	Type I-F	PS19	GGA	Canonical target	PF2266	This study
pPF1270	mCherry, Tc ^R , OriT	<i>P. atrosepticum</i>	Type I-F	PS19	GAA	Slipping proxy (-1 slip)	PF2414	This study
pPF1271	mCherry, Tc ^R , OriT	<i>P. atrosepticum</i>	Type I-F	PS19	GCA	Slipping proxy (-1 slip)	PF2415	This study
pPF1202	mCherry, Tc ^R , OriT	<i>P. atrosepticum</i>	Type I-F	PS19	GTA	Slipping proxy (-1 slip)	PF2265	This study
pPF1228	mCherry, Tc ^R , OriT	<i>Serratia</i>	Type I-E	PS1	CTT	Canonical target	PF2333	This study
pPF1232	mCherry, Tc ^R , OriT	<i>Serratia</i>	Type I-E	PS1	ACTT	Slipping proxy (+1 slip)	PF2337	This study
pPF1229	mCherry, Tc ^R , OriT	<i>Serratia</i>	Type I-E	PS1	CCTT	Slipping proxy (+1 slip)	PF2334	This study
pPF1231	mCherry, Tc ^R , OriT	<i>Serratia</i>	Type I-E	PS1	GCTT	Slipping proxy (+1 slip)	PF2336	This study
pPF1230	mCherry, Tc ^R , OriT	<i>Serratia</i>	Type I-E	PS1	TCTT	Slipping proxy (+1 slip)	PF2335	This study
pPF1272	mCherry, Tc ^R , OriT	<i>Serratia</i>	Type I-E	PS2	CTT	Canonical target	PF2417	This study
pPF1273	mCherry, Tc ^R , OriT	<i>Serratia</i>	Type I-E	PS2	ACTT	Slipping proxy (+1 slip)	PF2418	This study
pPF1274	mCherry, Tc ^R , OriT	<i>Serratia</i>	Type I-E	PS2	CCTT	Slipping proxy (+1 slip)	PF2419	This study
pPF1275	mCherry, Tc ^R , OriT	<i>Serratia</i>	Type I-E	PS2	GCTT	Slipping proxy (+1 slip)	PF2420	This study
pPF1276	mCherry, Tc ^R , OriT	<i>Serratia</i>	Type I-E	PS2	TCTT	Slipping proxy (+1 slip)	PF2421	This study

*The inserts to construct these plasmids were generated by a 2-round overlap PCR using multiple primers. Only the primers specific to each plasmid are shown here. Additional details are in **Table S6**.

Table S5: Plasmids expressing mini-CRISPR loci; related to Figure 5.

Name	Features	Host	System	Spacer	Target PAM	Description	Relevant primers	Reference
pPF1352	Km ^R , Tc ^R , OriT	<i>Serratia</i>	Type I-E	Control	N/A	Control spacer - does not target JS26	PF2611/PF2612	This study
pPF1337	Km ^R , Tc ^R , OriT	<i>Serratia</i>	Type I-E	Spacer 1	CTT	Canonical spacer targeting JS26	PF2535/PF2536	This study
pPF1335	Km ^R , Tc ^R , OriT	<i>Serratia</i>	Type I-E	Spacer 2	CTT	Canonical spacer targeting JS26	PF2531/PF2532	This study
pPF1336	Km ^R , Tc ^R , OriT	<i>Serratia</i>	Type I-E	Spacer 3	CTT	Canonical spacer targeting JS26	PF2533/PF2534	This study
pPF1338	Km ^R , Tc ^R , OriT	<i>Serratia</i>	Type I-E	Spacer 4	CTT	Canonical spacer targeting JS26	PF2597/PF2598	This study
pPF1341	Km ^R , Tc ^R , OriT	<i>Serratia</i>	Type I-E	Spacer 1	ACTT	+1 slipped spacer targeting JS26	PF2603/PF2604	This study
pPF1339	Km ^R , Tc ^R , OriT	<i>Serratia</i>	Type I-E	Spacer 2	CCTT	+1 slipped spacer targeting JS26	PF2599/PF2600	This study
pPF1340	Km ^R , Tc ^R , OriT	<i>Serratia</i>	Type I-E	Spacer 3	GCTT	+1 slipped spacer targeting JS26	PF2601/PF2602	This study
pPF1342	Km ^R , Tc ^R , OriT	<i>Serratia</i>	Type I-E	Spacer 4	TCTT	+1 slipped spacer targeting JS26	PF2605/PF2606	This study
pPF1354	Km ^R , Tc ^R , OriT	<i>Serratia</i>	Type I-F	Control	N/A	Control spacer - does not target JS26	PF2615/PF2616	This study
pPF1346	Km ^R , Tc ^R , OriT	<i>Serratia</i>	Type I-F	Spacer 1	GG	Canonical spacer targeting JS26	PF2585/PF2586	This study
pPF1343	Km ^R , Tc ^R , OriT	<i>Serratia</i>	Type I-F	Spacer 2	GG	Canonical spacer targeting JS26	PF2579/PF2580	This study
pPF1497	Km ^R , Tc ^R , OriT	<i>Serratia</i>	Type I-F	Spacer 3	GG	Canonical spacer targeting JS26	PF2872/PF2873	This study
pPF1349	Km ^R , Tc ^R , OriT	<i>Serratia</i>	Type I-F	Spacer 4	GG	Canonical spacer targeting JS26	PF2591/PF2592	This study
pPF1347	Km ^R , Tc ^R , OriT	<i>Serratia</i>	Type I-F	Spacer 1	GC	-1 slipped spacer targeting JS26	PF2587/PF2588	This study
pPF1348	Km ^R , Tc ^R , OriT	<i>Serratia</i>	Type I-F	Spacer 1	AGG	+1 slipped spacer targeting JS26	PF2589/PF2590	This study
pPF1345	Km ^R , Tc ^R , OriT	<i>Serratia</i>	Type I-F	Spacer 2	CGG	+1 slipped spacer targeting JS26	PF2583/PF2584	This study
pPF1498	Km ^R , Tc ^R , OriT	<i>Serratia</i>	Type I-F	Spacer 3	TGG	+1 slipped spacer targeting JS26	PF2874/PF2875	This study
pPF1499	Km ^R , Tc ^R , OriT	<i>Serratia</i>	Type I-F	Spacer 3	GT	-1 slipped spacer targeting JS26	PF2876/PF2877	This study
pPF1350	Km ^R , Tc ^R , OriT	<i>Serratia</i>	Type I-F	Spacer 4	GA	-1 slipped spacer targeting JS26	PF2593/PF2594	This study

Table S6: Oligonucleotides used in this study; related to STAR Methods.

Please see attached Excel file.